

DYADIC FACTORIZATION AND EFFICIENT INVERSION OF SPARSE POSITIVE DEFINITE MATRICES *

MICHAŁ KOS, KRZYSZTOF PODGÓRSKI, HANQING WU[†]

Abstract. In inverting large sparse matrices, the key difficulty lies in effectively exploiting sparsity during the inversion process. One well-established strategy is the nested dissection, which seeks the so-called sparse Cholesky factorization. We argue that the matrices for which such factors can be found are characterized by a hidden dyadic sparsity structure. This paper builds on that idea by proposing an efficient approach for inverting such matrices. The method consists of two independent steps: the first packs the matrix into a dyadic form, while the second performs a sparse (dyadic) Gram-Schmidt orthogonalization of the packed matrix.

The novel packing procedure works by recovering block-tridiagonal structures, focusing on aggregating terms near the diagonal using the l_1 -norm, which contrasts with traditional methods that prioritize minimizing bandwidth, i.e. the l_∞ -norm. The algorithm performs particularly well for matrices that can be packed into banded or dyadic forms which are moderately dense. Due to the properties of l_1 -norm, the packing step can be applied iteratively to reconstruct the hidden dyadic structure, which corresponds to the detection of separators in the nested dissection method.

We explore the algebraic properties of dyadic-structured matrices and present an algebraic framework that allows for a unified mathematical treatment of both sparse factorization and efficient inversion of factors. For matrices with a dyadic structure, we introduce an optimal inversion algorithm and evaluate its computational complexity.

The proposed inversion algorithm and core algebraic operations for dyadic matrices are implemented in the R package DyadiCarma, utilizing Rcpp and RcppArmadillo for high-performance computing. An independent R-based matrix packing module, supported by C++ code, is also provided.

Key words. matrix inversion, nested dissection, sparse Cholesky factorization, Gram-Schmidt orthogonalization, Gauss elimination method, band matrix, bandwidth minimization, positive definite matrix, undirected graph, dyadic algorithm

MSC codes. 15A09, 15A23, 68Q25, 68R10

1. Introduction. Inverting large sparse matrices is a classical computational challenge in high-dimensional statistical analysis, spatial econometrics, the numerical solution of algebraic and differential equations. The matrix inversion problem and its solution methods are intrinsically related to several classical algebraic techniques, such as least squares, Gauss elimination, Gram-Schmidt orthogonalization, and Cholesky factorization, among many others. If one relates this to elimination methods, the idea can be traced back not only to Sir Isaac Newton but also to ancient Chinese and Old Babylonian practices; see [10] for an engaging historical account. The connections, while often not spelled out, are quite straightforward, so we briefly account for them.

Computing the inverse of a matrix can be reinterpreted as finding a general solution in β to a linear equation

$$(1.1) \quad \mathbf{y} = \mathbf{X}\beta.$$

If the solution is unique, then any method of finding it, such as the Gauss elimination method, is simply a method of evaluation \mathbf{X}^{-1} at a specific \mathbf{y} . Finding $\mathbf{X}^{-1}\mathbf{y}$ is not the same as evaluating the entire matrix \mathbf{X}^{-1} , a more general problem we focus on

*Submitted to the editors June 10, 2025.

Funding: Krzysztof Podgórski acknowledges the financial support of the Swedish Research Council (VR) Grant DNR: 2020-05168.

[†]Department of Statistics, Lund University School of Economics and Management, Box 743, 220 07 Lund, Sweden (Michal.Kos@stat.lu.se, Krzysztof.Podgorski@stat.lu.se, Hanqing.Wu@stat.lu.se)

here. The method of least squares, for which Gauss is also credited, can be viewed as a generalization to the case when the solution of (1.1) cannot be found in the exact sense but instead one is settling for the solution $\hat{\beta}$ which minimizes the sum of squares of the entries of $\mathbf{y} - \mathbf{X}\beta$. Of course, if the exact unique solution exists, then the least squares is just another method of finding $\mathbf{X}^{-1}\mathbf{y}$. The least squares can be presented as

$$\hat{\beta} = (\mathbf{X}^\top \mathbf{X})^{-1} \mathbf{X}^\top \mathbf{y}$$

and the inversion of the original matrix \mathbf{X} reduces to finding the inverse of a positive definite (if the rank of \mathbf{X} is equal to the number of its columns) matrix $\Sigma = \mathbf{X}^\top \mathbf{X}$. It should also be noted that if one deals with a sparse linear equation, i.e. when \mathbf{X} is sparse, it may also (but does not need to) lead to a sparse Σ . These are the premises of this work in which the inversion of sparse positive definite matrices is considered. In the presented approach, the sparsity of Σ is assumed to be in a permuted dyadic form, which will be defined in the next section, and it is shown that if \mathbf{X} also has such form (in the vertical direction), then it results in the dyadic form of $\Sigma = \mathbf{X}^\top \mathbf{X}$. This is one of the consequences of Theorem 2.8 of Section 2. The other, more important ones are discussed next.

Since $\hat{\beta}$ is obtained by minimizing the squared Euclidean distance (the sum of squares), $\mathbf{X}\hat{\beta}$ represents the projection of \mathbf{y} to the linear space spanned by the columns of \mathbf{X} . Such a projection can be obtained by orthonormalizing the columns of \mathbf{X} . This can be formally stated as finding a matrix \mathbf{P} such that \mathbf{XP} is made of the orthonormal columns, i.e.

$$(1.2) \quad \mathbf{P}^\top \Sigma \mathbf{P} = \mathbf{I},$$

where $\Sigma = \mathbf{X}^\top \mathbf{X}$ and \mathbf{I} is the identity. Let us emphasize that \mathbf{P} is not unique and its chosen form is the key factor in connecting inversion, orthogonalization, and factorization. The direct consequences of (1.2) are

$$(1.3) \quad \mathbf{P}^{-1} = \mathbf{P}^\top \Sigma,$$

$$(1.4) \quad \Sigma^{-1} = \mathbf{P} \mathbf{P}^\top,$$

$$(1.5) \quad \Sigma = \mathbf{P}^{-1\top} \mathbf{P}^{-1},$$

$$(1.6) \quad \mathbf{X} = \mathbf{Q} \mathbf{P}^{-1},$$

where $\mathbf{Q} = \mathbf{XP}$ is the mentioned columnwise orthogonal matrix. These relations demonstrate that once \mathbf{P} is found, the inversion, projection, factorization, and the least squares are solved. When \mathbf{P} is computed via the Gram-Schmidt process, it is triangular, and its inverse $\mathbf{R} = \mathbf{P}^{-1}$ is also triangular. Consequently, (1.5) corresponds to Cholesky factorization and (1.6) to the QR decomposition; indeed, Gram-Schmidt orthogonalization can be interpreted as Gauss elimination applied to Σ , see [16]. It should be mentioned that the above equivalence of the solutions is meant only in the mathematical formulation, while computational efficiency may prefer one technique of computing, say, \mathbf{P} over another, see, for example, [12] for an elaborating account of the computational aspects of the Gram-Schmidt orthogonalization.

In [7], the nested dissection approach has been proposed for the so-called sparse Cholesky factorization. In short, this approach seeks a permutation that reorders the original sparse matrix to facilitate an efficient sparse triangular decomposition. Equivalently, the dissection process leads to (1.5) in which \mathbf{P}^{-1} is a permuted sparse triangular matrix. The nested dissection assures a large portions of zeros in Σ to be

The first of the two main contributions of this work is to explain the efficiency of the nested dissection method through the dyadic Gram-Schmidt orthogonalization, which can be viewed as representation (1.2) of the $d \times d$ dyadic matrix Σ using a sparse dyadic \mathbf{P} . The dyadic framework is more natural due to the recursive nature of the nested dissection. This allows the evaluation of the computational gains of the Gauss elimination method through calculation of the complexity of the dyadic telescoping Gram-Schmidt orthogonalization algorithm which is formulated in Theorem 2.8. The algorithm works efficiently for dyadic matrices and even faster for block-tridiagonal matrices with the $d \log d$ -type numerical complexity, which is given in Theorems 3.7 and 3.9.

The second contribution is a novel packing method that primarily aims at band and tridiagonal matrices. However, by utilizing the l_1 -norm, it facilitates the discovery of the separators. Finding the packing into the band matrix that is optimal in the bandwidth sense is a well-known NP -complete computational problem, which means that an algorithm providing an exact solution is expected to have more than a polynomial time, see [14]. Nevertheless, efficient algorithms providing approximate solutions have been studied, see, for example, [20] and references therein. Our method differs from the classical bandwidth minimization problem in two critical aspects. Firstly, we change the objective function from the l_∞ -norm to the l_1 -norm of the largest horizontal distances of nonzero terms from the diagonal. Secondly, the goal is to retrieve a dyadic structure rather than a band structure, which is less restrictive. These two changes in the approach to packing a matrix are working together to provide more

dense packing within a less restrictive matrix structure, i.e. it promotes dense packing near the diagonal while allowing individual rows to have nonzero elements that are far from the diagonal.

In order to have a better insight into the novelty of our approach, we provide some further details. The goal is to determine a permutation matrix π such that, for a positive definite matrix Σ , the permuted matrix $\tilde{\Sigma} = \pi^\top \Sigma \pi$ attains a dyadic form suitable for the dyadic factorization algorithm. The method is based on Theorem 4.5, which under certain conditions allows approximation of the distance between any pair of row indices for an unknown optimally permuted matrix $\tilde{\Sigma}$. Of key importance is that to determine the distance matrix approximation, we do not need any knowledge about the optimal permutation matrix $\tilde{\pi}$. From this perspective, the whole problem boils down to determining the approximately optimal permutation matrix based on a set of distance approximations $\{\hat{d}_{ij}\}$, where \hat{d}_{ij} is an approximation of $|\pi(i) - \pi(j)|$ and π denotes the optimal permutation matrix. To solve the above problem, we utilize the multidimensional scaling method (MDS), which transforms information regarding pairwise “distances” among a set of n objects into a configuration of n points mapped into a Cartesian space. When this space is one-dimensional, the configuration establishes the order between the points, and the sequence of point ranks provides an approximation of the optimal permutation.

The rest of the paper organizes as follows: In Section 2, we define the family of dyadic matrices and discuss their algebraic properties. Section 3 formulates the dyadic factorization algorithm and establishes complexity results. The novel packing algorithm is presented in Section 4, for which the simulation results are given in Section 5. Finally, we provide additional technical details in the appendix.

2. Dyadic matrices, their decompositions and inversions. In this section, we consider several subalgebras of the associative algebra $\mathcal{M}(d)$ of $d \times d$ matrices over \mathbb{R} . It is also important to consider the positive definite cone $\mathcal{PD}(d) \subset \mathcal{M}(d)$ of symmetric matrices whose eigenvalues are positive (gramians of d independent vectors in \mathbb{R}^d). These new subalgebras are characterized by dyadic structures of nonzero entries.

We start with the formal definitions and notation. For notational convenience, in the following discussion, we introduce the general concept of block-sparsity patterns. Let $\mathbf{1}_{s \times t}$, $s, t \in \mathbb{N}$ denote the $s \times t$ matrix of ones, $\mathbf{0}_{s \times t}$, $s, t \in \mathbb{N}$ denote an $s \times t$ zero matrix, and for any $s \in \mathbb{N}$, let $[s] = \{1, 2, \dots, s\}$.

DEFINITION 2.1. *Let $k, s, r \in \mathbb{N}$ with $k, s, r > 0$, and let $\mathcal{I} \subset [s] \times [r]$ be a set of indices. A $ks \times kr$ matrix \mathbf{A} is said to have the (regular) block-sparsity pattern*

$$\mathcal{A} = \{\mathcal{I}, k\},$$

if, when \mathbf{A} is partitioned into an $s \times r$ matrix of $k \times k$ blocks,

$$\mathbf{A} = \begin{bmatrix} \mathbf{A}_{1,1} & \cdots & \mathbf{A}_{1,r} \\ \vdots & \ddots & \vdots \\ \mathbf{A}_{s,1} & \cdots & \mathbf{A}_{s,r} \end{bmatrix},$$

we have $\mathbf{A}_{i,j} = \mathbf{0}_{k \times k}$ whenever $(i, j) \notin \mathcal{I}$. We refer to \mathcal{I} as the index set and k as the block size of \mathcal{A} , respectively. Furthermore, in this case, we write $\mathbf{A} \in \mathcal{A}$. When the block size k is irrelevant in the discussion, we may refer to \mathcal{I} alone as the block-sparsity pattern and write $\mathbf{A} \in \mathcal{I}$ instead of $\mathbf{A} \in \mathcal{A}$ with an implicitly understood block size k .

Remark 2.2. The concept of a block-sparsity pattern can be naturally generalized to irregular cases, where matrices partitioned into blocks of varying sizes or where the blocks are not necessarily square. However, for simplicity, we restrict our discussion to the regular case where all blocks are square and of the same size.

In what follows, if \mathbf{A} is a $ks \times kr$ matrix partitioned as in Definition 2.1 and $\mathcal{A} = \{\mathcal{I}, k\}$ is the corresponding block-sparsity pattern, we denote by

$$\mathbf{A}_{\mathcal{A}} : (i, j) \mapsto \mathbf{A}_{i,j}, \quad (i, j) \in \mathcal{I},$$

the mapping that assigns to each index pair its corresponding $k \times k$ block.

Similarly, if \mathbf{A} is an $m \times kr$ matrix, with m an arbitrary positive integer, partitioned into r consecutive blocks of k columns with $\mathcal{B} = \{\mathcal{J}, k\}, \mathcal{J} \subset [r]$, we define

$$\mathbf{A}_{\cdot, \mathcal{B}} : j \mapsto \mathbf{A}_{\cdot, j}, \quad j \in \mathcal{J},$$

as the mapping that assigns to each column block index its corresponding $m \times k$ submatrix. Likewise, if \mathbf{A} is a matrix partitioned into s consecutive blocks of k rows, we denote the corresponding mapping by $\mathbf{A}_{\mathcal{B}, \cdot}$, where $\mathcal{B} = \{\mathcal{J}, k\}, \mathcal{J} \subset [s]$.

When the block size k is not explicitly relevant in the discussion, we adopt the shorthand notation $\mathbf{A}_{\mathcal{I}}, \mathbf{A}_{\cdot, \mathcal{J}}$, and $\mathbf{A}_{\mathcal{J}, \cdot}$, omitting the explicit reference to k .

2.1. Regular completely dyadic matrices. Dyadically structured matrices can be defined for an arbitrary d , in this work we focus exclusively on the regular completely dyadic $d \times d$ matrices for which $d = k(2^N - 1)$, where $N, k \in \mathbb{N}$. In our framework, the dyadic structure is viewed as a block-sparsity pattern with a pyramidally constructed index set $\mathcal{D} \subset [2^N - 1]^2$ combined with a specified block size k . Here we refer to k as the *breadth* of a dyadic structure (to be defined) and N as its *height*. Let us define the following pyramid $\mathcal{P}(N)$ of height N , consisting of sets of integers

$$(2.1) \quad I_l = \bigcup_{r=1}^{2^{N-l}} I_{r,l} \quad \text{where } I_{r,l} = \{2^{l-1}(2r-1)\}, \quad l = 1, \dots, N$$

We refer to I_l as the l th level of the pyramid. With the pyramid of index sets $\mathcal{P}(N)$, one can also associate the pyramid $\mathcal{P}'(N)$ of index sets with levels $I'_l = \cup_r I'_{r,l}$ that are defined recursively as follows

$$(2.2) \quad \begin{aligned} I'_{r,1} &= I_{r,1}, \\ I'_{r,l} &= I_{r,l} \cup I'_{2r-1, l-1} \cup I'_{2r, l-1}, \quad r = 1, \dots, 2^{N-l}, l = 2, \dots, N. \end{aligned}$$

In fact, we can find an explicit decomposition of $I'_{r,l}$'s in terms of $I_{r,l}$. For $l \in 1, \dots, N$, the index set $I'_{r,l}$, $r \in 1, \dots, 2^{N-l}$ is made of consecutive integers decomposed as follows

$$(2.3) \quad \begin{aligned} I'_{r,l} &= \bigcup_{j=0}^{l-1} \bigcup_{m=1}^{2^j} I_{2^j(r-1)+m, l-j} = \\ &= 2^{l-1}(2r-1) + \{-2^{l-1}+1, \dots, -1, 0, 1, \dots, 2^{l-1}-1\}. \end{aligned}$$

This decomposition, which is a direct consequence of (2.2), is important for an efficient implementation of the algebra of dyadic matrices.

We now define the algebras that are made of various classes of dyadic matrices.

DEFINITION 2.3. Let $N, k \in \mathbb{N}, N, k > 0$. Consider the index set

$$\mathbf{I}_N = \bigcup_{l=1}^N \bigcup_{r=1}^{2^{N-l}} \mathbf{I}_{r,l} \subset [2^N - 1]^2,$$

where

$$\mathbf{I}_{r,l} = I_{r,l} \times I'_{r,l}.$$

We define the horizontally dyadic structure of height N and breadth k , denoted by $\mathcal{HD}(N, k)$, as the block-sparsity pattern given by \mathbf{I}_N and block size k . Similarly, let

$$\mathbf{I}_{r,l}^\top = \{(i, j) \in [2^N - 1]^2 : (j, i) \in \mathbf{I}_{r,l}\}, \quad r = 1, \dots, 2^{N-l}, l = 1, \dots, N.$$

The vertically dyadic structure of height N and breadth k , denoted by $\mathcal{VD}(N, k)$, is defined as the block-sparsity pattern given by the union of $\mathbf{I}_{r,l}^\top$'s and the block size k . Finally, the symmetrically dyadic structure $\mathcal{SD}(N, k)$ is defined as the union of $\mathbf{J}_{r,l} = \mathbf{I}_{r,l} \cup \mathbf{I}_{r,l}^\top$, $r = 1, \dots, 2^{N-l}$, $l = 1, \dots, N$.

A $d \times d$ matrix is called horizontally, vertically, or symmetrically dyadic if it has a block-sparsity pattern corresponding to $\mathcal{HD}(N, k)$, $\mathcal{VD}(N, k)$, or $\mathcal{SD}(N, k)$, respectively. For brevity, the corresponding classes of matrices are also denoted by $\mathcal{HD}(N, k)$, $\mathcal{VD}(N, k)$, and $\mathcal{SD}(N, k)$, with the context clarifying the intended meaning.

The dyadic structures can be identified with the respective matrices $\mathbf{H}(N, k)$, $\mathbf{V}(N, k)$, and $\mathbf{S}(N, k)$, which have 1's in all positions corresponding to potentially nonzero blocks. We also refer to symmetrically dyadic structures and matrices simply as dyadic. Moreover, we drop the explicit mention of k from the notation whenever its specific value is irrelevant.

Remark 2.4. In this work, for notational simplicity, we focus on the dyadic structures with uniform breadth both within and across levels, i.e., we consider only the regular block-sparsity patterns. However, the main ideas extend to more general dyadic structures, where the block size may vary and the structures may be incomplete when not all levels in the pyramid are fully populated. Although we do not consider this more general setup here, any irregular or incomplete dyadic matrix can be naturally embedded into a regular and complete one by filling in the blocks with identity matrix. Essentially, all the results can be generalized through this embedding. Some details on the embedding of irregular and incomplete dyadic matrices are presented in Appendix A.

Example 1. Let us consider $k \in \mathbb{N}$ and $N = 4$, then the block-sparsity pattern three types, horizontal, vertical, and symmetric, of dyadic structures are shown through * in the following matrices. In the dyadic matrix, to see the different dyadic structure levels, they are marked with different colors: the 1st level - black, the 2nd level - red, the 3rd level - green, and the fourth level - blue. For $\mathbf{S} = \mathbf{S}(N, k)$, $\mathbf{S}_{\mathbf{I}_{1,1}} = \mathbf{1}_{k \times k}$ and $\mathbf{S}_{\mathbf{J}_{1,2}}$ is made of five $k \times k$ matrices forming a cross marked in "red" at the top-left corner of the right-hand side matrix.

In the following results, we gather fundamental properties of the introduced classes of dyadic matrices.

THEOREM 2.5. *The classes $\mathcal{HD}(N)$, $\mathcal{VD}(N)$, $\mathcal{SD}(N)$ are linear spaces, and the first two are closed on the matrix multiplication and thus are (associative) sub-algebras of \mathcal{M}_d . Moreover,*

$$\mathcal{HD}(N)\mathcal{VD}(N) \subseteq \mathcal{SD}(N) = \begin{cases} \mathcal{HD}(N) + \mathcal{VD}(N), \\ \mathcal{HD}(N)\mathcal{SD}(N), \\ \mathcal{SD}(N)\mathcal{VD}(N). \end{cases}$$

Straightforward arguments are omitted for brevity.

Remark 2.6. It should be noted that $\mathcal{VD}(N)\mathcal{HD}(N)$ is not made of dyadic matrices in any sense.

The next result emphasizes the recurrent nature of the dyadic structures and connects them to grammian representation of the positive definite dyadic matrices.

PROPOSITION 2.7. *The following properties hold*

- i) Let $\Sigma = \mathbf{F}^\top \mathbf{F} \in \mathcal{SD}(N) \cap \mathcal{PD}(d)$ and define $\mathbf{F}_{r,l} = \mathbf{F}_{\cdot, I_{r,l}}$, $r = 1, \dots, 2^{N-l}$, $l = 1, \dots, N$. If $I'_{r,l} \cap I'_{r',l'} = \emptyset$, then the linear spaces spanned by columns of $\mathbf{F}_{r,l}$ and $\mathbf{F}_{r',l'}$ are orthogonal.
- ii) We have the following recursive relationship

$$\begin{aligned} \mathbf{H}(N+1, k) &= \begin{bmatrix} \mathbf{H}(N, k) & \mathbf{0}_{d \times k} & \mathbf{0}_{d \times d} \\ \mathbf{1}_{d \times d} & \mathbf{1}_{k \times k} & \mathbf{1}_{k \times d} \\ \mathbf{0}_{d \times d} & \mathbf{0}_{d \times k} & \mathbf{H}(N, k) \end{bmatrix} \\ \mathbf{V}(N+1, k) &= \begin{bmatrix} \mathbf{V}(N, k) & \mathbf{1}_{d \times k} & \mathbf{0}_{d \times d} \\ \mathbf{0}_{k \times d} & \mathbf{1}_{k \times k} & \mathbf{0}_{k \times d} \\ \mathbf{0}_{d \times d} & \mathbf{1}_{d \times k} & \mathbf{V}(N, k) \end{bmatrix} \\ \mathbf{S}(N+1, k) &= \begin{bmatrix} \mathbf{S}(N, k) & \mathbf{1}_{d \times k} & \mathbf{0}_{d \times d} \\ \mathbf{1}_{k \times d} & \mathbf{1}_{k \times k} & \mathbf{1}_{k \times d} \\ \mathbf{0}_{d \times d} & \mathbf{1}_{d \times k} & \mathbf{S}(N, k) \end{bmatrix}. \end{aligned}$$

- iii) If we remove the rows and columns from a dyadic matrix of height N that correspond to the index sets $I_{r,1}$ for $r = 1, \dots, 2^{N-1}$, the resulting matrix remains dyadic but with a reduced height of $N-1$.

If \mathbf{A} is a dyadic matrix of either type, then we identify it with a family of submatrices located by the index set of dyadic structures $\mathbf{A}_{\mathcal{I}}$. When there is a default dyadic structure involved, we do not distinguish between \mathbf{A} and $\mathbf{A}_{\mathcal{I}}$. The operation described in *iii*) is defined as a subsampling along $\tilde{\mathcal{I}} = \mathcal{HD}(N-1)$ and the resulting symmetric dyadic matrix is written simply as $\mathbf{A}_{\tilde{\mathcal{I}}}$. This naturally extends to any $\tilde{\mathcal{I}} = \mathcal{HD}(M)$ for any $M < N$.

In the following theorem, we present factorization results for symmetrically dyadic positive definite (PD) matrices. Since we deal with symmetric PD matrices, they can be only dyadic in symmetric structure and thus we drop the reference to symmetry and we refer simply to dyadic PD matrices. The algorithms delivering these factorizations efficiently are presented in the next section and their justification serves as a proof of the following result, see Lemma 3.2 and Theorem 3.7.

THEOREM 2.8. *Let $\Sigma \in \mathcal{SD}(N) \cap \mathcal{PD}(d)$, $d = k(2^N - 1)$. Then there exists $\mathbf{P} \in \mathcal{VD}(N)$ such that*

$$\mathbf{P}^\top \Sigma \mathbf{P} = \mathbf{I},$$

and $\mathbf{R} = \mathbf{P}^{-1} = \mathbf{P}^\top \boldsymbol{\Sigma} \in \mathcal{VD}(N)$.

COROLLARY 2.9. *With the notation of Theorem 2.8,*

$$\begin{aligned}\boldsymbol{\Sigma} &= \mathbf{R}^\top \mathbf{R}, \\ \boldsymbol{\Sigma}^{-1} &= \mathbf{P} \mathbf{P}^\top.\end{aligned}$$

Remark 2.10. In the proof that is presented in the Appendix, we utilize an unspecified orthogonalization $\mathbf{G}(\bar{\boldsymbol{\Sigma}})$ and can consider any generic algorithm that orthogonalizes a matrix $\bar{\mathbf{F}}$ of k columns such that $\bar{\boldsymbol{\Sigma}} = \bar{\mathbf{F}}^\top \bar{\mathbf{F}}$. The matrix \mathbf{P} in the above theorem depends only on $\mathbf{G}(\bar{\boldsymbol{\Sigma}})$ and is otherwise unique. A simple choice for $\mathbf{G}(\cdot)$ is the Gram-Schmidt method, but more refined and/or numerically stable methods can be considered in numerical implementations that are discussed in the next section.

Remark 2.11. It should be noted that $\boldsymbol{\Sigma}^{-1}$ does not need to be (and typically is not) a dyadic matrix.

3. Dyadic algorithm and its complexity. In this section, we provide details of an efficient algorithm that leads to the decomposition of Theorem 2.8. That is, for $\boldsymbol{\Sigma} \in \mathcal{SD}(N) \cap \mathcal{PD}(d)$, the algorithm returns a $\mathbf{P} \in \mathcal{VD}(N)$ satisfying

$$\mathbf{P}^\top \boldsymbol{\Sigma} \mathbf{P} = \mathbf{I}$$

Since the output is vertically dyadic, the algorithm computes the blocks $\mathbf{P}_{\mathcal{I}}$ with $\mathcal{I} = \mathcal{VD}(N)$, which uniquely determines \mathbf{P} .

The algorithm proceeds level-by-level for $l = 1, \dots, N$, computing these blocks through an iterative procedure that serves as an efficient non-recursive alternative to the recurrent approach presented in the proof of Theorem 2.8. Because this method specifically utilizes the dyadic structures, we refer to it as the dyadic algorithm. However, the overall scheme of the algorithm is a universal sequential orthogonalization, which computationally is equivalent to sparse Gaussian elimination or sparse Cholesky decomposition.

Efficient implementations of the dyadic algorithm for general symmetric dyadic matrices, an accelerated version for block-tridiagonal matrices, and the basic algebraic operations for dyadic matrices introduced in the previous section are provided in the R package `DyadiCarma`, which is publicly available¹. The package leverages Rcpp and RcppArmadillo to deliver high-performance computation in C++ while ensuring ease of use within the R environment.

To evaluate the complexity of the algorithm, we count the number of floating-point operations (flops). Typically, an addition, a multiplication, or a comparison is counted as one flop, while divisions, square roots, and exponentials are assigned a larger but constant cost [11]. However, following [19], we treat each of these operations as a single flop since this simplification does not affect the overall complexity in big- O notation. A similar complexity result was obtained in earlier works in the context of sparse Gaussian elimination [13, 17], providing corroboration for the optimality of the dyadic algorithm.

3.1. Sequential orthogonalization. The main idea of the dyadic algorithm is to use sequential orthogonalization, which can be viewed as an extension of the Gram-Schmidt method to dyadic groups of vectors

$$\mathbf{F}_l = [\mathbf{F}_{1,l} \quad \dots \quad \mathbf{F}_{2^{N-l},l}], \quad l = 1, \dots, N,$$

¹See Github repository: <https://github.com/Slangevar/DyadiCarma>

and to exploit numerical efficiencies inherent in the dyadic structures. However, the sequential orthogonalization method works for any $\mathbf{F} = [\mathbf{F}_1 \ \dots \ \mathbf{F}_N]$ and leads to \mathbf{P} in (3) for $\mathbf{\Sigma} = \mathbf{F}^\top \mathbf{F}$.

In this approach, we assume that each gramian $\mathbf{\Sigma}_{l,l} = \mathbf{F}_l^\top \mathbf{F}_l$ possesses a structure that allows for a generic orthonormalization procedure, which we denote by $\mathbf{G}_l(\cdot)$, where the argument is a positive definite matrix having the desired structure. It can then be shown (see Appendix B) that Algorithm 3.1 produces a matrix \mathbf{P} satisfying (3) as long as the matrices $\tilde{\mathbf{\Sigma}}$ evaluated in the loop have the structure that allows application of \mathbf{G}_l 's to evaluate \mathbf{G} shown in Algorithm 3.1.

Algorithm 3.1 Sequential orthogonalization $\mathbf{P}(\mathbf{\Sigma})$

INPUT: $\mathbf{\Sigma}$ corresponding to a $d \times d$ symmetrically dyadic matrix
 $\mathbf{P} = \mathbf{G}_1(\mathbf{\Sigma}_{1,1}); \{ \text{orthonormalization of } \mathbf{F}_1, \text{ i.e. } \mathbf{P}^\top \mathbf{F}_1^\top \mathbf{F}_1 \mathbf{P} = \mathbf{I} \}$
for $l = 2$ to N **do**
 $\tilde{\mathbf{\Sigma}} = \begin{bmatrix} \mathbf{\Sigma}_{1,l} \\ \vdots \\ \mathbf{\Sigma}_{l-1,l} \end{bmatrix}$
 $\tilde{\mathbf{\Sigma}}' = \mathbf{P}^\top \tilde{\mathbf{\Sigma}};$
 $\mathbf{A} = \mathbf{P} \tilde{\mathbf{\Sigma}}';$
 $\tilde{\mathbf{\Sigma}} = \mathbf{\Sigma}_{l,l} - \tilde{\mathbf{\Sigma}}'^\top \tilde{\mathbf{\Sigma}}';$
 $\mathbf{G} = \mathbf{G}_l(\tilde{\mathbf{\Sigma}});$
 $\mathbf{P} = \begin{bmatrix} \mathbf{P} & -\mathbf{A}\mathbf{G} \\ 0 & \mathbf{G} \end{bmatrix}; \{ \text{Orthonormalization of } [\mathbf{F}_1 \ \dots \ \mathbf{F}_l] \}$
end for
RETURN: \mathbf{P} orthogonalizing $\mathbf{\Sigma}$, as in factorization (3), corresponding to a vertically dyadic matrix

The following generic result about the complexity of the sequential orthogonalization is obvious.

PROPOSITION 3.1. *Let g_l be the complexity of evaluating $\mathbf{G}_l(\tilde{\mathbf{\Sigma}})$ for a specific matrix $\tilde{\mathbf{\Sigma}}$ and a_l, b_l, c_l, d_l are the costs of evaluating of $\mathbf{P}^\top \tilde{\mathbf{\Sigma}}, \mathbf{P} \tilde{\mathbf{\Sigma}}', \mathbf{\Sigma}_{l,l} - \tilde{\mathbf{\Sigma}}'^\top \tilde{\mathbf{\Sigma}}', \mathbf{A}\mathbf{G}$, respectively, at the l th step of the algorithm, then the total cost of the sequential orthogonalization algorithm is*

$$C = \sum_{l=1}^N g_l + \sum_{l=2}^N (a_l + b_l + c_l + d_l)$$

3.2. A dyadic implementation of the sequential orthogonalization. The main algorithm of this work utilizes sequential orthogonalization in the context of the symmetric dyadic matrices $\mathbf{\Sigma}$ that are gramians of

$$\mathbf{F} = [\mathbf{F}_1 \ \dots \ \mathbf{F}_N],$$

where $\mathbf{F}_l = [\mathbf{F}_{1,l} \ \dots \ \mathbf{F}_{2^{N-l},l}]$, $l = 1, \dots, N$ but considered in the dyadic order. The transfer from the sequential order to the dyadic one is represented by

$$\{1, \dots, 2^N - 1\} \ni i = 2^N(1 - 2^{-l+1}) + r \longleftrightarrow (r, l) \in \bigcup_{l=1}^N \{1, \dots, 2^{N-l}\} \times \{l\}.$$

Thus the sequential orthogonalization for dyadic matrices $\Sigma \in \mathcal{SD}(N)$ becomes dyadic one by utilizing one-to-one mapping between vectors in the sequential order to the dyadic order expressed in levels $l \in \{1, \dots, N\}$ and locations $r \in \{1, \dots, 2^{N-l}\}$ within the level l . This dyadic pyramid representation can be turned to the linear one using (2.1).

The well-established numerical complexity the Gram-Schmidt orthogonalization method applied to a $k \times k$ gramian matrix, is expressed by $O(k^3)$ flops. In the sequential algorithm that runs through levels of the dyadic pyramid, orthogonalization $\mathbf{G}_l(\cdot)$ is based on Gram-Schmidt orthogonalizations of $2^{N-l} k \times k$ submatrices from which $\tilde{\Sigma}$ is made at the diagonal (and zero otherwise). We conclude that in the complexity of Proposition 3.1:

$$\sum_{l=1}^N g_l = \sum_{l=1}^N 2^{N-l} O(k^3) = (2^N - 1) O(k^3) = O(dk^2).$$

Thus it is enough to discuss the remaining terms in the complexity formula of Proposition 3.1. With the same transfer scheme, matrix $\tilde{\Sigma}$ and matrix \mathbf{P} during the sequential orthogonalization will have specific block-sparsity patterns, namely $\mathcal{ED}(N, l)$ and $\mathcal{IVD}(N, l)$. A detailed discussion on these patterns will be given in the next section.

3.3. Numerical complexity of dyadic algebra. We define several specific sparsity patterns in connection to the matrices that will appear in the sequential orthogonalization. Thus, we consider the *diagonal block-sparsity pattern* of block size k for matrices of size $k2^{N-l} \times k2^{N-l}$, $l = 1, \dots, N$, which is given by

$$(3.1) \quad \mathcal{D}(N, l) = \{(i, j) : i \in [2^{N-l}], j = i\},$$

where, as before, $[s] = \{1, \dots, s\}$. Furthermore, the *elongated dyadic diagonal block-sparsity pattern* of block size k is defined for matrices of size $k(2^N - 2^{N-l+1}) \times k2^{N-l}$, $l = 2, \dots, N$, by

$$(3.2) \quad \mathcal{ED}(N, l) = \{(i, j) : j \in [2^{N-l}], i \in (j-1)(2^l - 2) + [2^l - 2]\}.$$

This pattern can be naturally interpreted as the block-sparsity pattern of the submatrix

$$(3.3) \quad \Sigma_{\mathcal{ED}}, \text{ where } \mathcal{ED} = \bigcup_{r=1}^{2^{N-l}} (\mathbf{I}_{r,l}^\top \setminus (I_{r,l} \times I_{r,l})) \text{ and } \Sigma \in \mathcal{SD}(N)$$

Define

$$(3.4) \quad \mathcal{ED}(N, l)_r = \{(i, r) : i \in (r-1)(2^l - 2) + [2^l - 2]\},$$

which identifies the elongated diagonal blocks indexed by $\mathbf{I}_{r,l}^\top \setminus (I_{r,l} \times I_{r,l})$ in the corresponding Σ in (3.3). If matrix $\mathbf{E} \in \mathcal{ED}(N, l)$, we can decompose it as

$$(3.5) \quad \mathbf{E} = \sum_{r=1}^{2^{N-l}} \mathbf{E}_r,$$

where \mathbf{E}_r has the block-sparsity pattern $\mathcal{ED}(N, l)_r$. This decomposition will be useful for complexity analysis.

Example 2. If a PD dyadic matrix $\Sigma = \mathbf{F}^\top \mathbf{F}$ and with the notation of Proposition 2.7, then the submatrix $\mathbf{F}_1^\top \mathbf{F}_2$ is $\mathcal{ED}(N, l)$ -elongated diagonal, where

$$\mathbf{F}_1 = [\mathbf{F}_{r,l'}]_{r=1, l'=1}^{2^{N-l}, l-1}, \quad \mathbf{F}_2 = [\mathbf{F}_{r,l}]_{r=1}^{2^{N-l}}.$$

The block matrices $[\mathbf{F}_{r,l'}]_{l'=1}^{l-1}^\top \mathbf{F}_{r,l}$ are the elongated diagonal blocks corresponding to $\mathcal{ED}(N, l)_r$, $r = 1, \dots, 2^{N-l}$.

Similarly, the incomplete dyadic block-sparsity pattern can be conveniently characterized by submatrices of Σ as in (3.3). For matrices of size $k(2^N - 2^{N-l+1}) \times k(2^N - 2^{N-l+1})$, $l = 2, \dots, N$, the *incomplete symmetrically dyadic block-sparsity pattern* of block size k , denoted by $\mathcal{IS}(N, l)$, is defined in accordance to the submatrix

$$\Sigma_{\mathcal{IS}}, \text{ where } \mathcal{IS} = \mathcal{SD}(N) \setminus \bigcup_{l'=l}^N \bigcup_{r=1}^{2^{N-l'}} \mathbf{J}_{r,l'}.$$

We observe that a matrix $\mathbf{S} \in \mathcal{IS}(N, l)$ is made of block-diagonal symmetrically dyadic submatrices, i.e.

$$(3.6) \quad \mathbf{S} = \sum_{r=1}^{2^{N-l+1}} \mathbf{S}_r,$$

where \mathbf{S}_r is $\mathcal{SD}(l-1)$ in the r -th diagonal $k(2^{l-1} - 1) \times k(2^{l-1} - 1)$ block and zero otherwise.

Following the same logic, we define level- l incomplete vertically dyadic block-sparsity pattern $\mathcal{IV}(N, l)$ and its horizontal counterpart $\mathcal{IH}(N, l)$ via

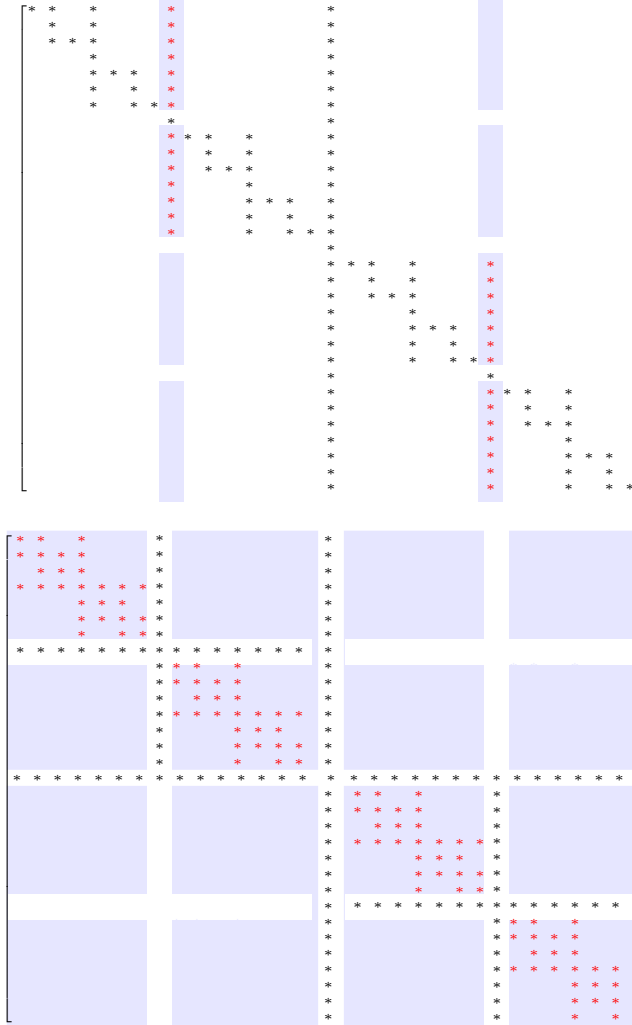
$$(3.7) \quad \mathcal{IV} = \mathcal{VD}(N) \setminus \bigcup_{l'=l}^N \bigcup_{r=1}^{2^{N-l'}} \mathbf{I}_{r,l'}^\top, \quad \mathcal{IH} = \mathcal{HD}(N) \setminus \bigcup_{l'=l}^N \bigcup_{r=1}^{2^{N-l'}} \mathbf{I}_{r,l'}.$$

As with $\mathcal{VD}(N)$ and $\mathcal{HD}(N)$, if a matrix $\mathbf{V} \in \mathcal{IV}(N, l)$, then $\mathbf{V}^\top \in \mathcal{IH}(N, l)$, and vice versa. Moreover, if matrices $\mathbf{V} \in \mathcal{IV}(N, l)$ and $\mathbf{H} \in \mathcal{IH}(N, l)$, then we can decompose them into block diagonal matrices

$$(3.8) \quad \mathbf{V} = \sum_{r=1}^{2^{N-l+1}} \mathbf{V}_r, \quad \mathbf{H} = \sum_{r=1}^{2^{N-l+1}} \mathbf{H}_r,$$

where the block-sparsity pattern of each \mathbf{V}_r (respectively, \mathbf{H}_r) is given by $\mathcal{VD}(l-1)$ (respectively, $\mathcal{HD}(l-1)$) in the r -th diagonal block of size $k(2^{l-1} - 1)$ and zero elsewhere.

Example 3. Let $N = 5$ and $l = 4$, then the elongated diagonal $\mathcal{ED}(5, 4)$ and bottom-up incomplete symmetrically dyadic structures $\mathcal{IS}(5, 4)$ are shown with red stars and light-blue background within the complete vertical and symmetrically dyadic matrices, respectively. Similarly as before, each $*$ represents $\mathbf{1}_{k \times k}$.



The following lemma summarizes the complexity of evaluating products of incomplete dyadic, elongated diagonal, and block diagonal matrices. They are crucial for establishing the main complexity result of this section. A straightforward proof is given in Appendix B.

LEMMA 3.2. *Let $\mathbf{H} \in \mathcal{IH}(N, l)$, $\mathbf{V} \in \mathcal{IV}(N, l)$, $\mathbf{D} \in \mathcal{D}(N, l)$, and $\mathbf{E} \in \mathcal{ED}(N, l)$. Then $\mathbf{HE} \in \mathcal{ED}(N, l)$ and $\mathbf{VE} \in \mathcal{ED}(N, l)$, and the computation of either of these two products requires $O(ldk^2)$ flops, while $\mathbf{E}^\top \mathbf{E} \in \mathcal{D}(N, l)$ and $\mathbf{ED} \in \mathcal{ED}(N, l)$, and the computation of either of these two products requires $O(dk^2)$ flops.*

Next, we gather some basic facts about algebraic operations on matrices having dyadic structures and evaluate associated numerical complexities.

Suppose that $\mathbf{H} \in \mathcal{HD}(N)$, $\mathbf{V} \in \mathcal{VD}(N)$, and $\mathbf{S} \in \mathcal{SD}(N)$. Then we have the following decomposition

$$\mathbf{H} = \sum_{l=1}^N \sum_{r=1}^{2^{N-l}} \mathbf{H}_{\mathbf{J}_{r,l}}, \quad \mathbf{V} = \sum_{l=1}^N \sum_{r=1}^{2^{N-l}} \mathbf{V}_{\mathbf{J}_{r,l}}, \quad \mathbf{S} = \sum_{l=1}^N \sum_{r=1}^{2^{N-l}} \mathbf{S}_{\mathbf{J}_{r,l}},$$

where the matrices in the sum have the same size as the left-hand-side matrices and have block-sparsity pattern indicated by the index sets.

Let us recall that the computation of the product of two $k \times k$ matrices involves $O(k^3)$ flops, while adding them requires $O(k^2)$ flops.

PROPOSITION 3.3. *Let $\mathbf{S} \in \mathcal{SD}(N)$ and \mathbf{A} is a $d \times k$ matrix. Then*

$$\mathbf{SA} = \sum_{l=1}^N \sum_{r=1}^{2^{N-l}} \mathbf{S}_{\mathbf{J}_{r,l}} \mathbf{A}_{I'_{r,l}},$$

and its computation involves $O(dk^2 \log(d/k))$ flops.

Proof. The equation is obvious thus to obtain the computational cost it is enough to find out the cost of multiplying symmetric cross-matrix $\mathbf{S}_{\mathbf{J}_{r,l}}$ by $\mathbf{A}_{I'_{r,l}}$. It involves multiplications of two $k \times k$ matrices and then adding the results. In terms of complexity, we only need to consider the number of such multiplications, which is essentially the number of nonzero blocks in the cross-matrix $\mathbf{S}_{\mathbf{J}_{r,l}}$. There are $2^{l+1} - 3$ nonzero blocks in $\mathbf{S}_{\mathbf{J}_{r,l}}$. As a result, the total number of such matrix multiplications is

$$\begin{aligned} \sum_{l=1}^N \sum_{r=1}^{2^{N-l}} (2^{l+1} - 3) &= (2N - 3)2^N + 3 \\ &= O(N2^N) \end{aligned} \quad (3.9)$$

Hence, the total number of flops required is

$$\begin{aligned} O(k^3 N 2^N) &= O\left(k^3 \left(\frac{d}{k} + 1\right) \log\left(\frac{d}{k} + 1\right)\right) \\ &= O\left(dk^2 \log\left(\frac{d}{k}\right)\right). \end{aligned} \quad (3.10) \quad \square$$

PROPOSITION 3.4. *Let $\mathbf{V} \in \mathcal{VD}(N)$ and \mathbf{A} is a $d \times k$ matrix. Then*

$$\mathbf{VA} = \sum_{l=1}^N \sum_{r=1}^{2^{N-l}} \mathbf{V}_{\mathbf{I}_{r,l}^\top} \mathbf{A}_{I'_{r,l}},$$

and its computation involves $O(dk^2 \log(d/k))$ flops.

Proof. The argument is almost identical to that for Proposition 3.3, except that now we are consider the column-matrix instead of cross-matrix. There are $2^l - 1$ nonzero blocks in $\mathbf{V}_{\mathbf{I}_{r,l}^\top}$, and the total number of multiplication of two $k \times k$ matrices are

$$\begin{aligned} \sum_{l=1}^N \sum_{r=1}^{2^{N-l}} (2^l - 1) &= N2^N - 2^N + 1 \\ &= O(N2^N), \end{aligned} \quad (3.11)$$

and the number of flops required is $O(dk^2 \log(d/k))$. \square

Symmetrically, with almost the same reasoning, we have

PROPOSITION 3.5. *Let $\mathbf{H} \in \mathcal{HD}(N)$ and \mathbf{A} is a $d \times k$ matrix. Then*

$$\mathbf{H}\mathbf{A} = \sum_{l=1}^N \sum_{r=1}^{2^{N-l}} \mathbf{H}_{\mathbf{I}_{r,l}} \mathbf{A}_{I'_{r,l}}.$$

and its computation involves $O(dk^2 \log(d/k))$ flops.

The following result is tightly connected to the complexity of inverting dyadic matrices through Theorem 2.8.

THEOREM 3.6. *It takes $O(d^2k)$ flops to compute $\mathbf{P}\mathbf{Q}^\top$, where $\mathbf{P}, \mathbf{Q} \in \mathcal{VD}(N, k)$ and $d = k(2^N - 1)$.*

Proof. We prove the result by mathematical induction, analyzing the recurrence for the number a_N of flops needed for the multiplication.

For $N = 1$, the matrices \mathbf{P} and \mathbf{Q} are, in general, dense $k \times k$ matrices, so their product requires $a_1 = Ck^3$ flops for some constant $C > 0$.

For $N > 1$, the recursive relationship in iii) of Proposition 2.7 indicates the following sparsity patterns of products. Consequently, all blocks in $\mathbf{P}\mathbf{Q}^\top$ are potentially nonzero and the corresponding products of blocks need to be evaluated

$$\begin{aligned} & \mathbf{V}(N+1, k) \mathbf{V}(N+1, k)^\top \\ &= \begin{bmatrix} \mathbf{V}(N, k) \mathbf{V}(N, k)^\top + \mathbf{1}_{d \times k} \mathbf{1}_{k \times d} & \mathbf{1}_{d \times k} \mathbf{1}_{k \times k} & \mathbf{1}_{d \times k} \mathbf{1}_{k \times d} \\ \mathbf{1}_{k \times k} \mathbf{1}_{k \times d} & \mathbf{1}_{k \times k} \mathbf{1}_{k \times k} & \mathbf{1}_{k \times d} \\ \mathbf{1}_{d \times k} \mathbf{1}_{k \times d} & \mathbf{1}_{d \times k} \mathbf{1}_{k \times k} & \mathbf{V}(N, k) \mathbf{V}(N, k)^\top + \mathbf{1}_{d \times k} \mathbf{1}_{k \times d} \end{bmatrix}. \end{aligned}$$

It is thus easy to see the following recursive relationship

$$\begin{aligned} a_{N+1} &= 2a_N + C [4(2^N - 1)^2 + 4(2^N - 1) + 1] k^3 \\ &= 2a_N + C (2^{N+1} - 1)^2 k^3, \end{aligned}$$

which leads to

$$\begin{aligned} a_N &= Ck^3 \sum_{K=1}^N 2^{N-K} (2^K - 1)^2 \\ &= Ck^3 2^N \sum_{K=1}^N \left(2^{-K/2} - 2^{K/2} \right)^2 = Ck^3 (2^N (2^{N+1} - 2N - 1) - 1). \end{aligned}$$

In particular, since $d = k(2^N - 1)$, we have $a_N = O(d^2k)$. \square

3.4. Complexity of the dyadic algorithm. In this section, we justify the efficiency of our dyadic algorithm by obtaining its numerical complexity.

THEOREM 3.7. *Let $\mathbf{\Sigma} \in \mathcal{SD}(N)$. Algorithm 3.1 requires $O(dk^2 \log^2(d/k))$ flops to obtain the corresponding matrix $\mathbf{P} \in \mathcal{VD}(N)$.*

Proof. As discussed in Section 3.2, the Gram-Schmidt orthonormalization process in total costs $O(dk^2)$ flops.

For $l = 2, \dots, N$, Algorithm 3.1 performs the following matrix computations: $\mathbf{P}^\top \check{\mathbf{\Sigma}}$, $\mathbf{P} \check{\mathbf{\Sigma}}'$, $\mathbf{\Sigma}_{l,l} - \check{\mathbf{\Sigma}}'^\top \check{\mathbf{\Sigma}}'$, and $\mathbf{A}\mathbf{G}$. We analyze these computations one by one, repeatedly invoking Lemma 3.2.

Let us consider the case for a given value of l . First, for

$$\check{\mathbf{\Sigma}}' = \mathbf{P}^\top \check{\mathbf{\Sigma}},$$

we have $\mathbf{P}^\top \in \mathcal{IH}(N, l)$ and $\check{\mathbf{\Sigma}} \in \mathcal{ED}(N, l)$. Hence, $\check{\mathbf{\Sigma}}' \in \mathcal{ED}(N, l)$, and this operation requires $O(ldk^2)$ flops. Second, for

$$\mathbf{A} = \mathbf{P}\check{\mathbf{\Sigma}}',$$

we obtain $\mathbf{A} \in \mathcal{ED}(N, l)$ with a cost of $O(ldk^2)$ flops. Next, for

$$\tilde{\mathbf{\Sigma}} = \mathbf{\Sigma}_{l,l} - \check{\mathbf{\Sigma}}'^\top \check{\mathbf{\Sigma}}',$$

it has been shown that this step incurs $O(dk^2)$ flops and that $\tilde{\mathbf{\Sigma}} \in \mathcal{D}(N, l)$. Lastly, \mathbf{G} is obtained by orthonormalizing $\tilde{\mathbf{\Sigma}}$ so that $\mathbf{G} \in \mathcal{D}(N, l)$, and it takes $O(dk^2)$ flops to calculate \mathbf{AG} .

Therefore, for a given $l \geq 2$, the number of flops required for the corresponding step of Algorithm 3.1 is

$$O(ldk^2) + O(ldk^2) + O(dk^2) + O(dk^2) = O(ldk^2)$$

Taking the complexity of the Gram-Schmidt orthonormalization into consideration, the overall number of flops required by Algorithm 3.1 is

$$\begin{aligned} \sum_{l=2}^N O(ldk^2) &= O(dk^2 N^2) \\ &= O(dk^2 \log^2(d/k)). \end{aligned} \quad \square$$

A notable subclass of symmetric dyadic matrices, $\mathcal{SD}(N) \cap \mathcal{PD}(d)$, is the class of *block-tridiagonal matrices* with block size k . These matrices are composed of $k \times k$ blocks arranged in a tridiagonal pattern, one along the main diagonal with the block super-diagonal and sub-diagonal. This subclass includes $d \times d$ *band matrices*, which are explicitly defined in Section 5.

When $\mathbf{\Sigma}$ is block-tridiagonal, for each $l = 2, \dots, N$ the sparsity patterns of $\check{\mathbf{\Sigma}}$ and $\check{\mathbf{\Sigma}}'$ can be refined. Define

$$s(j, l) = (2^{l-1} - 1)(2j - 1), \quad 1 \leq j \leq 2^{N-l}.$$

Then, in iteration l ,

$$\widetilde{\mathcal{ED}}(N, l) = \{(i, j) : 1 \leq j \leq 2^{N-l}, s(j, l) \leq i \leq s(j, l) + 1\}$$

describes the block-sparsity pattern of $\check{\mathbf{\Sigma}}$. Moreover, if we let

$$\mathcal{T}(l) = \{-2^{l-m} + 1 : m = 2, \dots, l\} \cup \{2^{l-m} : m = 2, \dots, l\},$$

then it is shown in Lemma 3.8 that, in iteration l , the block-sparsity pattern of $\check{\mathbf{\Sigma}}'$ is

$$\widetilde{\mathcal{ED}}'(N, l) = \{(i, j) : 1 \leq j \leq 2^{N-l}, i = s(j, l) + t, t \in \mathcal{T}(l)\}.$$

In this refined setting, the overall complexity of the dyadic algorithm can be reduced by a factor of $\log(d/k)$.

LEMMA 3.8. Let $\mathbf{H} \in \mathcal{IH}(N, l)$, $\mathbf{V} \in \mathcal{IV}(N, l)$, and $\mathbf{E} \in \widetilde{\mathcal{ED}}(N, l)$. Then $\mathbf{HE} \in \widetilde{\mathcal{ED}}'(N, l)$ and $\mathbf{VHE} \in \mathcal{ED}(N, l)$. Moreover, the computation of either of these two products requires $O(dk^2)$ flops.

THEOREM 3.9. If Σ is a block-tridiagonal matrix with block size k , then Algorithm 3.1 requires $O(dk^2 \log(d/k))$ flops to obtain the corresponding matrix $\mathbf{P} \in \mathcal{VD}(N)$.

Proof. According to Lemma 3.8, in this case, for each $l = 2, \dots, N$, only $O(dk^2)$ flops will be required to calculate $\mathbf{P}^\top \tilde{\Sigma}$ and $\mathbf{P} \tilde{\Sigma}'$. As a result, the total number of flops required by Algorithm 3.1 under this special circumstance is

$$\sum_{l=2}^N O(dk^2) = O(dNk^2) = O(dk^2 \log(d/k)) \quad \square$$

4. Packing sparse matrices. We present a method of packing sparse matrices into the block-tridiagonal matrix and investigate how this process can be used to recursively retrieve the dyadic structure. In short, the main challenge is to find, for a given positive definite $d \times d$ -matrix Σ , a permutation matrix π such that $\pi^\top \Sigma \pi$ has a block-tridiagonal form to which the dyadic factorization algorithm applies. In practice, since the breadth of the sought dyadic (block-tridiagonal) matrix is not known a priori, we consider here an incomplete and possibly irregular dyadic (block-tridiagonal) structure.

For the purposes of this and the next sections, it matters only if the entries of Σ are zero or nonzero. Thus from now on, it is assumed that Σ is a symmetric 0 – 1 matrix, i.e. having 0 or 1 as its entries. Additionally, we assume that Σ cannot be represented as a block-diagonal matrix with more than one block. Otherwise, one could identify the individual blocks and perform the analysis separately on each of them, which would not affect the generality of our considerations.

Moreover, for a permutation π , the matrix representing it is denoted by π , i.e.

$$\pi = [\delta_{i\pi(j)}]_{i,j=1}^d,$$

where $\delta_{k,j} = 1$ if $k = j$ and zero otherwise. Since any $d \times d$ matrix is formally a block-tridiagonal matrix with one $d \times d$ block, our objective is to find a permutation π which optimally (in a certain sense) packs the nonzero entries close to the diagonal.

4.1. Optimal permutation. The essence of the dyadic algorithm is to optimally use the knowledge of zero blocks located at specific distances from the diagonal of the Σ matrix. In the following definition, we introduce a criterion for permutation optimality (4.1) that favors permutations placing nonzero elements near the diagonal.

DEFINITION 4.1. For a symmetric zero-one matrix Σ , a permutation π , and row indices i, j , we call

- $D_i = \{j : \Sigma_{i,j} \neq 0\}$ – the i -th neighborhood, i.e. the set of neighbors of the row index i ,
- $l_i^{(\pi)} = \max\{|\pi(i) - \pi(j)| : j \in D_i\}$ – the half-width of D_i under π ,
- $\|\mathbf{l}^{(\pi)}\|_1 = \sum_{i=1}^d l_i^{(\pi)}$ – the half-width of Σ under π ,
- a permutation π optimal if it is an element of the following set

$$(4.1) \quad \Pi(\Sigma) = \underset{\pi}{\operatorname{argmin}} \|\mathbf{l}^{(\pi)}\|_1.$$

Algorithm 4.1 Extracting configuration from the permutation distance matrix

INPUT: $\mathbf{G}_\pi = [G_{ij}]$ - $d \times d$ distance matrix associated with a permutation π
 $\alpha(1) = \min\{i : \#\{j : G_{ij} = 1\} = 1\}$; {Two i's satisfying the condition}
 $\alpha(2) = \text{find}(i : G_{i,\alpha(1)} = 1)$; {Only one i satisfies the condition}
 $m = 2$;
while $m < d$ **do**
 $\alpha(m+1) = \text{find}(i \neq \alpha(m-1) : G_{i,\alpha(m)} = 1)$; {Only one i satisfies the condition}
 $m = m + 1$
end while
 RETURN: α - a permutation that has the distance matrix \mathbf{G}_π

Since exactly solving (4.1) is computationally unfeasible, our goal is to approximate the optimal permutation. Our proposed approach leverages the relationship between the optimal permutation and its associated distance matrix.

4.2. Distance matrices. Distance matrices are widely used in modern multivariate data analysis and serve as a central component of our approach. For a set of distinct points $\mathbf{x} = (x_1, \dots, x_d)$ in a metric space (\mathcal{S}, ρ) , let

$$\mathbf{G}_{\rho, \mathbf{x}} = [\rho(x_i, x_j)]_{i,j=1}^d.$$

The focus is to reconstruct \mathbf{x} based on the distance matrix $\mathbf{G}_{\rho, \mathbf{x}}$.

When the points are real numbers, a simple algorithm can reconstruct them up to translation and reflection. The algorithm is based on the following partial information extracted from the $d \times d$ matrix $\mathbf{G}_{\mathbf{x}} = [|x_i - x_j|]_{i,j=1}^d$. For each i , let us determine a pair $\{j_i^1, j_i^2\}$ of indices corresponding to the two closest neighbors such that x_i sits in between them, i.e. the pair j_i^1, j_i^2 such that

$$|x_{j_i^1} - x_{j_i^2}| = |x_{j_i^1} - x_i| + |x_i - x_{j_i^2}|$$

and $|x_{j_i^1} - x_{j_i^2}|$ is the smallest among all pairs that satisfy the above. Such pairs exist for all i 's except the two that correspond to the endpoints of the range of \mathbf{x} . The information extracted from $\mathbf{G}_{\mathbf{x}}$ can be summarized as

$$\mathcal{I}(\mathbf{G}_{\mathbf{x}}) = \{\{j_e^1, j_e^2\} \subseteq \{1, \dots, d\}, \{(j_i^1, \rho_i^1), (j_i^2, \rho_i^2)\}, i \in \{1, \dots, d\} \setminus \{j_e^1, j_e^2\}\},$$

where j_e^1, j_e^2 are the indices of the endpoints of the range of \mathbf{x} , $\rho_i^1 = |x_{j_i^1} - x_i|$, $\rho_i^2 = |x_{j_i^2} - x_i|$. The algorithm that reconstructs \mathbf{x} using only the information in $\mathcal{I}(\mathbf{G}_{\mathbf{x}})$ is detailed in Appendix B, and it serves as the proof of the following theorem.

THEOREM 4.2. *Let $\mathbf{x} \in \mathbb{R}^d$ be such that $x_i \neq x_j$ for all $i \neq j$, and define the matrix $\mathbf{G}_{\mathbf{x}} = [|x_i - x_j|]_{i,j=1}^d$. Then there exists $\mathbf{y} \in \mathbb{R}^d$ that depends on $\mathbf{G}_{\mathbf{x}}$ only through $\mathcal{I}(\mathbf{G}_{\mathbf{x}})$ such that $\mathbf{G}_{\mathbf{y}} = \mathbf{G}_{\mathbf{x}}$. Moreover, there exists $s \in \mathbb{R}$ such that either $\mathbf{x} = s + \mathbf{y}$ or $\mathbf{x} = s - \mathbf{y}$.*

Remark 4.3. It follows from Theorem 4.2 that the distance matrix $\mathbf{G}_{\mathbf{x}}$ that contains d^2 entries is fully recovered from $\mathcal{I}(\mathbf{G}_{\mathbf{x}})$ that involves only $4d - 6$ entities. These entities represent information about two neighbors: the one closest on the right and the one closest on the left, without specifying which is which.

Let us consider now the distance matrix associated with a permutation π :

$$\mathbf{G}_\pi = [\|\pi(i) - \pi(j)\|]_{i,j=1}^d.$$

For this special case, Theorem 4.2 reconstructs a permutation γ for which the distance matrix coincides with \mathbf{G}_π . Moreover, $\mathcal{I}(\mathbf{G}_\pi)$ does not need to include ρ_i^1 's and ρ_i^2 's since they are equal to one. Thus, one needs only $2d - 2$ values describing the closest neighbors

$$\mathcal{I}(\mathbf{G}_\pi) = \{\{j_e^1, j_e^2\} \subseteq \{1, \dots, d\}, \{j_i^1, j_i^2\}, i \in \{1, \dots, d\} \setminus \{j_e^1, j_e^2\}\}.$$

The straightforward algorithm in this case is presented in Algorithm 4.1.

There are two possible scenarios, either $\gamma = \pi$ when $\pi(\alpha(1)) = 1$, or $\gamma = \rho \circ \pi$ when $\pi(\alpha(1)) = d$, where ρ is a permutation such that $\rho(i) = \rho(d + 1 - i)$ (for $i = 1, 2, \dots, d$). The above result indicates that when only the distance matrix \mathbf{G}_π is known, it is possible to determine the associated permutation, up to a certain transformation. However, in light of the formulated optimization problem (4.1), it is easy to observe that if the permutation π is optimal, then the permutation $\rho \circ \pi$ is also optimal. This is related to the simple fact that relabeling given by the permutation ρ preserves the half-widths of sets D_i . More precisely, for any symmetric matrix $\mathbf{\Sigma}$, any permutation π , and any index i , the half-width of D_i under π and under $\rho \circ \pi$ is the same. Consequently, knowing the distance matrix for an optimal permutation allows us to determine an optimal permutation. The following conclusion summarizes the relationship between the distance matrix and its associated permutation.

Remark 4.4. Let \mathbf{G}_π be the distance matrix associated with an unknown permutation π . Based on the matrix \mathbf{G}_π , it is possible to determine two permutations, π and $\rho \circ \pi$, without knowing which corresponds to the original. Furthermore, the permutation π is optimal if and only if $\rho \circ \pi$ is also optimal.

We conclude this section with an overview of the fundamental concepts behind the classical Multidimensional Scaling (MDS) method. This approach is also commonly referred to as Principal Coordinates Analysis, Torgerson Scaling or Torgerson–Gower Scaling, [18, 9]. Classical MDS aims to find a configuration of d points in a p -dimensional Euclidean space represented as rows in $\mathbf{X} \in \mathbb{R}^{d \times p}$, $d > p$, such that the pairwise distances between them approximate the original distances given in the $d \times d$ distance matrix \mathbf{G} , see Algorithm 4.2.

The rationale behind the algorithm can be easily explained in the special case when the initial matrix \mathbf{G} is made of the Euclidean distances, i.e. the distances are between vectors that are rows in a $d \times d$ matrix \mathbf{Y} , i.e. $\mathbf{G}_{ij} = \|\mathbf{Y}_{i\cdot} - \mathbf{Y}_{j\cdot}\|$ (additionally let $\mathbf{K} = [\mathbf{G}_{ij}^2]$). Clearly, for $\mathbf{\Sigma} = \mathbf{Y}\mathbf{Y}^\top$ and $d \times 1$ matrix $\mathbf{1}$ of ones

$$(4.2) \quad \mathbf{K} = \mathbf{1} \operatorname{diag}(\mathbf{\Sigma})^\top + \operatorname{diag}(\mathbf{\Sigma}) \mathbf{1}^\top - 2\mathbf{\Sigma}.$$

Here, $\operatorname{diag}(\cdot)$ extracts the diagonal vector from a matrix argument, or creates a diagonal matrix from a vector argument. If each of the columns is recentered by a constant, then \mathbf{G} does not change. Consequently, from now on one can assume that the columns of \mathbf{Y} are centered at zero, i.e. $\mathbf{\Sigma}\mathbf{1} = \mathbf{1}^\top\mathbf{\Sigma} = \mathbf{0}$. We observe also that $\mathbf{H}\mathbf{1} = \mathbf{1}^\top\mathbf{H} = \mathbf{0}$ so that, with the notation of Algorithm 4.2, we have

$$\begin{aligned} \mathbf{H}\mathbf{K}\mathbf{H} &= \mathbf{H}\mathbf{1} \operatorname{diag}(\mathbf{\Sigma})^\top \mathbf{H} + \mathbf{H} \operatorname{diag}(\mathbf{\Sigma}) \mathbf{1}^\top \mathbf{H} - 2\mathbf{H}\mathbf{\Sigma}\mathbf{H} \\ &= -2\mathbf{\Sigma} + \frac{2}{d} (\mathbf{1}\mathbf{1}^\top \mathbf{\Sigma} + \mathbf{\Sigma}\mathbf{1}\mathbf{1}^\top) - \frac{2}{d^2} \mathbf{1}\mathbf{1}^\top \mathbf{\Sigma} \mathbf{1}\mathbf{1}^\top \\ &= -2\mathbf{\Sigma}. \end{aligned}$$

Algorithm 4.2 Classical multidimensional scaling

INPUT: $\mathbf{G} = [G_{ij}]$ - $d \times d$ symmetric matrix of distances; $p < d$ - reduced dimension

$\mathbf{K} = [G_{ij}^2]$; {Compute the squared distance matrix}

$\mathbf{H} = \mathbf{I} - \frac{1}{d}\mathbf{1}\mathbf{1}^\top$; {1 - the column vector of 1's }

$\mathbf{B} = -\mathbf{H}\mathbf{K}\mathbf{H}/2$; {Double-centering}

$(\mathbf{\Lambda}, \mathbf{V}) = \text{eigen}(\mathbf{B})$; {Decreasing eigenvalues, and the corresponding eigenvectors}

$\mathbf{\Lambda}_p = \mathbf{\Lambda}[1:p]$; {The p -largest eigenvalues, assumed to be positive}

$\mathbf{V}_p = \mathbf{V}[1:p]$; {The corresponding eigenvectors}

RETURN: $\mathbf{X}_p = \mathbf{V}_p \text{diag}(\mathbf{\Lambda}_p)^{1/2}$ - The d rows are p -dimensional configuration vectors with distances approximating the ones in \mathbf{G} .

From this, we observe that \mathbf{B} in the algorithm is equal to nonnegative definite $\mathbf{\Sigma}$ and since $\mathbf{\Sigma} = \mathbf{V}\mathbf{\Lambda}\mathbf{V}^\top$ thus $\mathbf{\Sigma} - \mathbf{X}_p\mathbf{X}_p^\top$ is also nonnegative definite having the sum of eigenvalues (trace norm) equal to $\lambda_{p+1} + \dots + \lambda_d$, where $\mathbf{\Lambda} = (\lambda_1, \dots, \lambda_d)$. Consequently, replacing in (4.2), $\mathbf{\Sigma}$ by $\mathbf{X}_p\mathbf{X}_p^\top$ leads to a good approximation $\mathbf{G}_p = \|\mathbf{X}_{p;i} - \mathbf{X}_{p;j}\|$ of \mathbf{G} with the error controlled by $\lambda_{p+1} + \dots + \lambda_d$. When \mathbf{G} is not generated by Euclidean distances, the error analysis is no longer straightforward. For a more detailed and comprehensive description of the method, readers are referred to [1].

The most computationally intensive part of classical MDS is the eigendecomposition of the $d \times d$ matrix \mathbf{B} , which has a complexity of $O(d^3)$ (for details see e.g. [19]). Additionally, storing the \mathbf{K} and \mathbf{B} matrices requires $O(d^2)$ memory. This makes classical MDS infeasible for very large datasets. To address these limitations, several algorithms have been developed: Divide-and-Conquer MDS and Interpolation MDS, see [5], FastMap, see [6], Fast Multidimensional Scaling (Fast MDS), see [22], Landmark Multidimensional Scaling (Landmark MDS or LMDS), see [4], MetricMap, see [21], Pivot MDS, see [2], and Reduced MDS, see [15].

These methods can be applied to our problem; however, they predominantly assume that distances between all points are well-approximated. This condition is too restrictive, since our focus is only on distances to close neighbors. As shown in subsequent sections, our method approximates the distance matrix \mathbf{G}_π associated with the optimal permutation. The method approximates all elements of \mathbf{G}_π well only if \mathbf{G}_π belongs to a relatively narrow class of matrices. Crucially, for a significantly broader class of matrices, our approximation provides a good estimate of distances between close neighbors while underestimating the true distances between points that are far apart. On the other hand, in light of Remark 4.3, a good approximation of distances between close neighbors appears to be sufficient to obtain reliable results. Based on this observation, we have developed a dedicated algorithm that determines the positions of points based primarily on nearest-neighbor distances.

4.3. The approximate distance matrix optimization method. In this section, we outline the core ideas of our method, which consist of the following two steps

- *Approximating the optimal permutation distance matrix.* The key property behind our method is that the elements of the approximating distance matrix are completely independent of the choice of permutation. More precisely,

constructing the proximate distance matrix does not require knowledge of the optimal permutation and is only based on the sets of neighbors.

- *Approximating the optimal permutation using the approximation matrix.* Our approximation matrix is a distance matrix, but it uses a non-Euclidean distance. Consequently, the method of reconstructing points on the real line described in the previous section cannot be applied. Instead, we use the multidimensional scaling. The MDS transforms the approximation distance matrix to a one-dimensional space, where the resulting configuration defines an ordering of the points, and the sequence of point ranks provides an approximation to the optimal permutation.

Clearly, the distance matrix \mathbf{G}_π associated with the optimal permutation π requires prior knowledge of the optimal permutation itself. However, even without explicit information about the optimal permutation, it is possible to approximate the elements of \mathbf{G}_π by utilizing the information about the neighbor sets. For a given $\Sigma \in \mathcal{PD}(d)$, we define the approximation as the distance matrix

$$(4.3) \quad \mathbf{A}_\Sigma = \left[\frac{|D_i \Delta D_j|}{2} \right]_{i,j=1}^d,$$

where $|D_i \Delta D_j|$ is the number of elements in the symmetric difference of sets, which is a metric on the space of all subsets of $\{1, \dots, d\}$. We demonstrate that, under certain conditions, \mathbf{A}_Σ serves as a good approximation of \mathbf{G}_π for the optimal π . This is mathematically argued in Theorem 4.5 and the subsequent conclusions.

A simple measure of the proximity of two matrices is the average absolute difference between the corresponding entries. However, as we have seen in the previous section, determining the permutation π does not require knowledge of all elements of the distance matrix \mathbf{G}_π . It is sufficient to know the nearest neighbor on each side of the point corresponding to a given row (see Remark 4.3). Therefore, we consider the following criteria

$$(4.4) \quad \delta_m(\mathbf{G}_\pi, \mathbf{A}_\Sigma) = \frac{1}{dm} \sum_{\substack{i,j=1 \\ [\mathbf{G}_\pi]_{ij} \leq m}}^d \left| [\mathbf{G}_\pi]_{ij} - [\mathbf{A}_\Sigma]_{ij} \right|.$$

The restriction $[\mathbf{G}_\pi]_{ij} \leq m$ means that we consider only nearest neighbors at a distance no greater than m (when $m = d$ we consider all elements). We are interested in determining the following set of permutations

$$(4.5) \quad B_{\Sigma,m} = \operatorname{argmin}_{\pi} \delta_m(\mathbf{G}_\pi, \mathbf{A}_\Sigma).$$

Ideally, we would like to know whether the optimal permutation is in $B_{\Sigma,m}$, which will make \mathbf{A}_Σ a good candidate for approximation. Such a strong result is unknown, but we instead derive an upper bound for $\delta_m(\mathbf{G}_\pi, \mathbf{A}_\Sigma)$ which takes the minimal value for the optimal π , see Remarks 4.10 and 4.12 below. In the following theorem and proposition, we use the notation of Subsection 4.1. The proof of the theorem can be found in Appendix B.

THEOREM 4.5. *Let Σ be a symmetric 0–1 matrix and π be a permutation. Suppose i and j is a pair of two different row indices such that*

$$(4.6) \quad |l_i^{(\pi)} - l_j^{(\pi)}| \leq [\mathbf{G}_\pi]_{ij} \leq l_i^{(\pi)} + l_j^{(\pi)}.$$

Then

$$(4.7) \quad \left| [\mathbf{G}_\pi]_{ij} - [\mathbf{A}_\Sigma]_{ij} \right| \leq \frac{(2l_i^{(\pi)} + 1 - |D_i|) + (2l_j^{(\pi)} + 1 - |D_j|)}{2}.$$

Since the assumptions (4.6) involve the unknown $l_i^{(\pi)}$ and $l_j^{(\pi)}$, it is practical to establish an alternative condition that directly implies these relations. The following proposition provides a sufficient condition for the right-hand side assumption.

PROPOSITION 4.6. *For a permutation π and indices i and j :*

$$D_i \cap D_j \neq \emptyset \Rightarrow [\mathbf{G}_\pi]_{ij} \leq l_i^{(\pi)} + l_j^{(\pi)}.$$

Proof. Let $t \in D_i \cap D_j \neq \emptyset$. By the definition of half-width

$$[\mathbf{G}_\pi]_{ij} = |\pi(i) - \pi(j)| \leq |\pi(i) - \pi(t)| + |\pi(t) - \pi(j)| \leq l_i^{(\pi)} + l_j^{(\pi)}.$$

The advantage of condition $D_i \cap D_j \neq \emptyset$ is that it is easy to check and does not reference the optimal permutation. Furthermore, the condition has clear interpretation (rows i and j must have a common neighbor). However, this condition is rather restrictive, as only relatively close rows can satisfy it (in the following section, we discuss how this limitation can be circumvented). When the condition is not satisfied, $[\mathbf{A}_\Sigma]_{ij}$ can be significantly smaller than $[\mathbf{G}_\pi]_{ij}$ as illustrated in the following example.

Example 4. For full symmetric tridiagonal matrices, the set of optimal permutations consists of two elements: the identity permutation and permutation ρ , defined as $\rho(i) = \rho(d+1-i)$ for $i = 1, 2, \dots, d$. Moreover, the following relations hold

i) For any pair i, j ,

$$[\mathbf{A}_\Sigma]_{ij} = \frac{|D_i \triangle D_j|}{2} \leq \frac{(|D_i| + |D_j|)}{2} \leq 3.$$

ii) For any optimal permutation π , if $\pi(i), \pi(j) \notin \{1, d\}$ and $D_i \cap D_j \neq \emptyset$, then $[\mathbf{G}_\pi]_{ij} = [\mathbf{A}_\Sigma]_{ij}$.

From i), even for a moderate d , many pairs of indices i, j will satisfy $[\mathbf{G}_\pi]_{ij} = |\pi(i) - \pi(j)| > [\mathbf{A}_\Sigma]_{ij}$. On the other hand, ii) shows that the approximation is exact for closest neighbors.

Remark 4.7. Mathematically, the condition $D_i \cap D_j \neq \emptyset$ is sufficient for the right-hand side assumption to hold. However, in practice, relying on the approximation when the condition is not fulfilled appears unreasonable, as it may result in a significant underestimation of $[\mathbf{G}_\pi]_{ij}$. Notably, the condition is guaranteed for elements i and j of any nearest neighbors set D_r , since $i, j \in D_r$ implies $r \in D_i \cap D_j$. Furthermore, as shown in the procedure for determining the permutation based on the distance matrix, information about the nearest neighbors is sufficient (see Remark 4.3).

Now, let us consider the assumption on the left-hand side of (4.6). Since $[\mathbf{G}_\pi]_{ij} = |\pi(i) - \pi(j)|$, the above condition compares two distances. Unfortunately, there is no simple alternative to replace this assumption. Nevertheless, if the optimal permutation leads to a dense block-tridiagonal matrix, it is reasonable to assume that the parameters $l_i^{(\pi)}$ and $l_j^{(\pi)}$ are either similar, relatively small, or both. In such cases, the left-hand side is expected to be small.

The upper bound (4.7) is an average of two terms, each corresponding to a different row. To better understand the factors influencing this bound, we introduce the concept of density for the sets involved.

From the definition of $l_i^{(\pi)}$, it follows that

$$\pi(D_i) \subseteq \pi(i) + C(l_i^{(\pi)}),$$

where $C(t) = \{-t, \dots, -1, 0, 1, \dots, t\}$. The cardinalities of these sets are $|D_i|$ and $2l_i^{(\pi)} + 1$, respectively, with the obvious inequality $|D_i| \leq 2l_i^{(\pi)} + 1$.

To quantify how densely the set $\pi(D_i)$ is distributed within $\pi(i) + C(l_i^{(\pi)})$, we define the density measure

$$\eta_i(\pi) = \frac{|D_i|}{2l_i^{(\pi)} + 1}.$$

This quantity satisfies $\frac{1}{2l_i^{(\pi)} + 1} \leq \eta_i(\pi) \leq 1$, where values closer to 1 indicate a higher density of elements from $\pi(D_i)$ in the given range. This allows for density comparisons across different indices on the same scale.

To assess the overall density across all rows, we define the mean density

$$\bar{\eta}(\pi) = \frac{1}{n} \sum_{i=1}^n \eta_i(\pi).$$

The density measure $\eta_i(\pi)$ leads to the following important observation.

Remark 4.8. The upper bound (4.7) decreases as the densities $\eta_i(\pi)$ and $\eta_j(\pi)$ increase. In other words, the denser $\pi(D_i)$ and $\pi(D_j)$ are within their respective intervals $\pi(i) + C(l_i^{(\pi)})$ and $\pi(j) + C(l_j^{(\pi)})$, the closer $[\mathbf{A}_\Sigma]_{ij}$ and $[\mathbf{G}_\pi]_{ij}$ become. In the extreme case where $\eta_i(\pi) = 1$ and $\eta_j(\pi) = 1$, we obtain exact equality

$$[\mathbf{A}_\Sigma]_{ij} = [\mathbf{G}_\pi]_{ij}.$$

Thus, the density measure $\eta_i(\pi)$ enables consistent comparisons across different indices and is directly related to the accuracy of the approximation (4.7).

The repeated use of inequalities (4.7) applied to the formula (4.4) for $\delta_d(\mathbf{G}_\pi, \mathbf{A}_\Sigma)$ leads to

$$\begin{aligned} d^2 \delta_d(\mathbf{G}_\pi, \mathbf{A}_\Sigma) &\leq \sum_{i=1}^d \sum_{j=1, j \neq i}^d (l_i^{(\pi)} + l_j^{(\pi)}) + \sum_{i=1}^d \sum_{j=1, j \neq i}^d \left(1 - \frac{|D_i| + |D_j|}{2}\right) = \\ &= 2(d-1) \|\mathbf{l}^{(\pi)}\|_1 + \sum_{i=1}^d \sum_{j=1, j \neq i}^d \left(1 - \frac{|D_i| + |D_j|}{2}\right), \end{aligned}$$

which establishes the following result.

PROPOSITION 4.9. *Let $\Sigma \in \mathcal{PD}(d)$ and π be a permutation. If (4.6) is satisfied for any pair of row indices $i, j \in \{1, \dots, d\}$, then*

$$\delta_d(\mathbf{G}_\pi, \mathbf{A}_\Sigma) \leq Q(\pi, \Sigma),$$

$$\text{where } Q(\pi, \Sigma) = \frac{2(d-1)}{d^2} \|\mathbf{l}^{(\pi)}\|_1 + \frac{1}{d^2} \sum_{i=1}^d \sum_{j=1, j \neq i}^d \left(1 - \frac{|D_i| + |D_j|}{2}\right)$$

Remark 4.10. We highlight two key observations.

1. The upper bound $Q(\pi, \Sigma)$ consists of two components. The first one is the scaled half-width of the Σ matrix under the permutation π , while the second component is independent of the choice of permutation. Consequently,

$$\operatorname{argmin}_{\pi} Q(\pi, \Sigma) = \operatorname{argmin}_{\pi} \|\mathbf{l}^{(\pi)}\|_1.$$

The above equation shows that the distance $\delta_d(\mathbf{G}_{\pi}, \mathbf{A}_{\Sigma})$ has the tightest upper bound $Q(\pi, \Sigma)$ for the optimal permutation.

2. The upper bound $Q(\pi, \Sigma)$ is the sum of bounds (4.7) over all pairs indices $i \neq j$. In light of Remark 4.8, if for the permutation π , the mean $\bar{\eta}(\pi)$ is close to 1, which means that sets $\pi(D_i)$ are on average dense in the corresponding intervals $\pi(i) + C(l_i^{(\pi)})$, then $Q(\pi, \Sigma)$ should be relatively close to 0.

Given the above observations, we can see that the matrix \mathbf{A}_{Σ} is a good candidate for the approximation of \mathbf{G}_{π} associated with the optimal permutation π , at least when certain conditions are met.

In Proposition 4.9, we assumed that (4.6) holds for all pairs of indices. As demonstrated earlier, this assumption is quite restrictive (see Example 4). Let us now consider the case where the condition is satisfied only for the closest neighbors.

PROPOSITION 4.11. *Let π be a permutation. Suppose that (4.6) is satisfied for any pair of row indices $i, j \in \{1, \dots, d\}$ such that $[\mathbf{G}_{\pi}]_{ij} \leq m$ for some natural number m . Then the following inequality holds*

$$\begin{aligned} \delta_m(\mathbf{G}_{\pi}, \mathbf{A}_{\Sigma}) &\leq \frac{4}{d} \|\mathbf{l}^{(\pi)}\|_1 + \frac{2}{d} \sum_{i=1}^d (1 - |D_i|) \\ &\quad - \frac{1}{d} \left(\sum_{\pi(i)=1}^m \frac{m+1-\pi(i)}{m} \left(2l_i^{(\pi)} + 1 - |D_i| \right) \right. \\ &\quad \left. + \sum_{\pi(i)=d-m+1}^d \frac{m-d+\pi(i)}{m} \left(2l_i^{(\pi)} + 1 - |D_i| \right) \right) \end{aligned}$$

The proof of this proposition is in Appendix B.

Remark 4.12. The formula for the upper bound is noticeably more complex compared to $Q(\pi, \Sigma)$, however, when $m = d$, they coincide. On the other hand, when m/d is small (corresponding to the case of primary interest where only the closest neighbors are considered) then the negative term is also negligible. Thus it is reasonable to expect that the upper bound from Proposition 4.11 is the smallest for a permutation close to the optimal permutation (see observation 1 in Remark 4.10).

Since the upper bound from Proposition 4.11 is nearly equivalent to the sum of the bounds (4.7) (on proper combinations of indices), it follows that point 2 from Remark 4.10 generalizes to the considered scenario. More precisely, when the mean density $\bar{\eta}(\pi)$ is close to 1, the upper bound has to be close to 0, and the matrices \mathbf{A}_{Σ} and \mathbf{G}_{π} associated with optimal permutation are close in the metric δ_m when m is relatively small in comparison to d .

Remark 4.13. The condition of matrix proximity is primarily a theoretical requirement. Simulations indicate that even when $\bar{\eta}(\pi)$ deviates significantly from 1, our method, which relies on the approximation matrix \mathbf{A}_{Σ} , still produces permutations close to the optimal for a broad class of matrices. This suggests that the method is fairly robust to violations of this condition.

4.4. Algorithm. As mentioned earlier, classical MDS is not suitable for large matrices, and existing algorithms addressing this limitation typically require the distance matrix to accurately reflect relationships between all pairs of points. In contrast, we assume that $\mathbf{A} = \mathbf{A}_\Sigma$ provides a good approximation only for elements that are close to each other. Consequently, while existing methods remain applicable, they are unlikely to yield accurate results in this setting. However, Remark 4.3 suggests that knowing distances between nearest neighbors is sufficient to determine the configuration of points. Motivated by this, we present an algorithm that computes the configuration of points based solely on the distances between their nearest neighbors. Without delving into technical details, the algorithm has a three-step process.

We extract indices on which the permutation will be built (SKELETON), attach to them the local configurations (FLESH), and use these to build the global configuration (BODY). A more detailed breakdown of these components is provided below.

SKELETON: A subset of strategically chosen row indices $J = \{i_1, i_2, \dots, i_{|J|}\}$, selected based on a criterion discussed later.

FLESH: A collection of local configurations, where for each $i \in J$, the classical MDS determines the arrangement of points in D_i using the corresponding submatrix of \mathbf{A} . These local configurations will later be used to construct the full permutation.

BODY: A global configuration and the associated permutation, assembled from local configurations. Since the local configurations are determined only up to translation and reflection, alignment along the skeleton J is required.

4.4.1. Local configurations. The selection of elements in J is closely tied to the alignment process used for the final configuration. Therefore, we first focus on local configurations (FLESH). Here, we apply classical MDS on sets D_i , for all $i \in J$. More precisely, let $D_i = \{m_1, \dots, m_{s_i}\}$, where $m_k < m_{k+1}$. Based on the neighborhoods of the elements in D_i , we calculate distance matrices

$$[\mathbf{A}^{(i)}]_{kj} = \frac{|D_{m_k} \Delta D_{m_j}|}{2}, \quad k, j \in \{1, \dots, s_i\}.$$

Next, we apply classical MDS to obtain a one-dimensional configuration vector $\mathbf{x}^{(i)} \in \mathbb{R}^{s_i}$, where $x_k^{(i)}$ represents the position of row index $m_k \in D_i$ on a line, as determined by classical MDS. The reason for using $\mathbf{A}^{(i)}$ is to effectively use the approximation (4.7). As discussed, it is beneficial that $D_{m_k} \cap D_{m_j} \neq \emptyset$ and, by Remark 4.7, this condition holds for any pair of elements within any nearest neighbor set D_i . For this reason, we treat the sets D_i , $i \in J$, as fundamental building blocks where classical MDS provides a reliable configuration of points.

4.4.2. Global configuration. Each vector $\mathbf{x}^{(i)}$ contains only partial information about the positions of indices, since it captures only relative relationships within D_i . To obtain a global configuration from this “flesh”, we unify information in all \mathbf{x}_i ’s utilizing the “skeleton” J .

We define the $d \times |J|$ matrix $\mathbf{Y} = [y_{ij}] = [\mathbf{y}_{\cdot j}]$, which encodes local configurations for indices $i_1, i_2, \dots, i_{|J|} \in J$. Each entry is given by

$$y_{m_k j} = \begin{cases} x_k^{(i_j)}, & \text{if } m_k \in D_{i_j} \\ 0, & \text{otherwise,} \end{cases}$$

where $x_k^{(i_j)}$ is the position on a line of a row index $m_k \in D_{i_j}$. The alignment process iteratively transforms subsequent columns $[\mathbf{y}_{\cdot j}]$ of the matrix \mathbf{Y} and stores the results

Algorithm 4.3 Flesh-to-body

INPUT: $\mathbf{Y} = [y_{ij}] = [\mathbf{y}_{\cdot j}]$ - $d \times J$ local configurations (columnwise) along the skeleton

$\tilde{\mathbf{Y}}_1 = [\mathbf{y}_{\cdot 1}]$; {Initiation of a new configuration matrix}

for $k = 2$ to J **do**

$(\hat{a}, \hat{b}) = \underset{(a,b) \in \{-1,1\} \times \mathbb{R}}{\operatorname{argmin}} f(a, b; \mathbf{y}_{\cdot k}, \tilde{\mathbf{Y}}_{k-1})$; {The objective function in (4.8)}

$\tilde{\mathbf{Y}}_k = [\tilde{\mathbf{Y}}_{k-1} \hat{a}\mathbf{y}_{\cdot k} + \hat{b}\mathbf{1}]$; {Adding the k-th column}

end for

$\mathbf{x} = \text{repeat}(\text{NA}, d)$; {Initiation of the final configuration vector}

$\mathbf{1} = \text{repeat}(1, J)$; {Column vector of ones}

for $k = 1$ to d **do**

$n = |\{j; \tilde{y}_{kj} \neq 0\}| > 0$;

if $n > 0$ **then**

$x_k = \tilde{\mathbf{y}}_{k \cdot} \mathbf{1} / n$; {Averaging nonzero entries in the rows}

end if

end for

RETURN: $\mathbf{x} = (x_k)_{k=1}^d$ - The global configuration along the skeleton based on \mathbf{Y} .

of iterations in a matrix $\tilde{\mathbf{Y}}$. In the algorithm, the first configuration vector $\tilde{\mathbf{y}}_{\cdot 1}$ is set to the original $\mathbf{y}_{\cdot 1}$. Then the subsequent configuration $\tilde{\mathbf{y}}_{\cdot k}$ given the previous $\tilde{\mathbf{Y}}_{k-1} = [\tilde{\mathbf{y}}_{\cdot i}]_{i < k}$ is obtained through minimizing in $(a, b) \in \{-1, 1\} \times \mathbb{R}$ the following objective function

$$\begin{aligned}
 (4.8) \quad f(a, b; \mathbf{y}_{\cdot k}, \tilde{\mathbf{Y}}_{k-1}) &= \sum_{m=1}^{k-1} \sum_{z=1}^d (\tilde{y}_{zm} - ay_{zk} - b)^2 \mathbb{I}(z \in D_{i_m} \cap D_{i_k}) \\
 &= \sum_{m=1}^{k-1} \|\mathbf{P}_{D_{i_m} \cap D_{i_k}} (\tilde{\mathbf{y}}_{\cdot m} - a\mathbf{y}_{\cdot k} - b\mathbf{1})\|_2^2,
 \end{aligned}$$

where, $Z \subseteq \{1, \dots, d\}$, \mathbf{P}_Z is a $d \times d$ diagonal matrix such that $P_{jj;Z} = \mathbb{I}(j \in Z)$.

As seen in Algorithm 4.3, the unified configuration vector \mathbf{x} is obtained by row-wise averaging local configurations given by $\tilde{\mathbf{Y}}$, ensuring optimal alignment along the skeleton. For $k \in \bigcup_{j=1}^{|J|} D_{i_j}$, the entries x_k of the configuration vector \mathbf{x} can be written somewhat more explicitly

$$x_k = \sum_{j=1}^{|J|} \tilde{y}_{kj} \mathbb{I}(k \in D_{i_j}) / \sum_{j=1}^{|J|} \mathbb{I}(k \in D_{i_j}).$$

If the index k does not belong to any of the sets D_{i_j} , the corresponding element in the configuration \mathbf{x} is unavailable, which should be prevented by a proper choice of the skeleton J . Below, we describe the conditions that the set J must satisfy to avoid this problem. If \mathbf{x} is fully determined, we approximate the optimal permutation as $\hat{\pi} = (r_1(\mathbf{x}), \dots, r_d(\mathbf{x}))$, where $r_i(\mathbf{x})$ denotes the position of x_i in the ordered sequence.

Remark 4.14. We now examine the objective function given in (4.8). This function measures the alignment of a new vector with previously modified vectors after reflection a and translation b , but only over the indices common to D_{i_k} and D_{i_m} . The optimization procedure seeks to find the transformation ensuring the best fit to prior data in the least-squares sense. This procedure is closely related to the Procrustes transformation, which aligns two point sets in Euclidean space using translation, scaling, and rotation to minimize the sum of squared distances between corresponding points. See [1] for details. For $k = 2$, our procedure is a special case of the Procrustes transformation, involving only translation and reflection in one dimension. For $k > 2$, it extends this idea to multiple vectors.

By solving the least-squares optimization, the optimal estimators are given by (4.9)

$$\hat{a} = \text{sign} \left(\sum_{j=1}^{k-1} \sum_{s \in D_{i_j} \cap D_{i_k}} \left(\tilde{y}_{sj} - \frac{\sum_{m=1}^{k-1} \sum_{z \in D_{i_m} \cap D_{i_k}} \tilde{y}_{zm}}{\sum_{m=1}^{k-1} |D_{i_m} \cap D_{i_k}|} \right) \left(y_{sk} - \frac{\sum_{m=1}^{k-1} \sum_{z \in D_{i_m} \cap D_{i_k}} y_{zk}}{\sum_{m=1}^{k-1} |D_{i_m} \cap D_{i_k}|} \right) \right)$$

$$\hat{b} = \frac{\sum_{m=1}^{k-1} \sum_{z \in D_{i_m} \cap D_{i_k}} (\tilde{y}_{zm} - \hat{a} y_{zk})}{\sum_{m=1}^{k-1} |D_{i_m} \cap D_{i_k}|}.$$

4.4.3. The choice of skeleton. The choice of skeleton J is crucial and serves as the first step of the algorithm. The main challenge is to find a skeleton which has sufficient overlaps between the neighborhoods of its element when the matrix is sparse. The following method does not assume any specific matrix structure, except that all rows are connected. We select the skeleton J that satisfies the following key criteria, ordered by importance.

Complete skeleton neighborhoods: The skeleton neighborhoods cover all indices, i.e.

$$\bigcup_{j \in J} D_j = \{1, 2, \dots, d\}.$$

Robust estimators: The estimator \hat{a} calculated at each step of alignment is robust, i.e. there is sufficient overlap between the skeleton neighborhoods.

Computational complexity and accuracy: The calculation of the estimators should be efficient, balancing complexity and accuracy. The set J should be as small as possible to reduce computational cost.

The first criterion must be satisfied, as failing to do so would leave some points without assigned positions in the global configuration vector, making the final permutation incomplete. Increasing the number of elements in the skeleton always ensures that this criterion is met, even for very sparse matrices. However, the challenge is not just satisfying this criterion but also ensuring sufficient overlap between the neighborhoods of skeleton elements, which is associated with the second criterion.

The second criterion is critical for achieving a high-quality approximation to the optimal permutation. Simulations indicate that an incorrect estimation of the parameter a can result in a permutation π where the half-width of Σ under π is significantly larger than in the optimal case. See Example 5 for further discussion. In this context, by analyzing the objective function from the alignment process (4.8), it is easy to notice that for every $r \geq 2$, a necessary condition for uniquely determining the

estimators is

$$(4.10) \quad \sum_{m=1}^{r-1} |D_{i_m} \cap D_{i_r}| \geq 2.$$

The necessity of Condition (4.10) arises from the fact that two parameters need to be estimated. If Condition (4.10) is not satisfied, at most one observation is available, making unique estimation impossible. Moreover, a stronger condition enhances robustness: for each r , having at least two different indices in $D_{i_r} \cap \bigcup_{m=1}^{r-1} D_{i_m}$ leads to more stable estimators in the alignment step. This stronger condition holds when i_r is a direct neighbor of a previous skeleton element i_m ($m < r$), since $i_r, i_m \in D_{i_m} \cap D_{i_r}$.

However, if the elements of the skeleton are not direct neighbors, they may only be connected through a common neighbor outside the skeleton, in which case the sum in (4.10) may be equal to one. This occurs in Example 4 with a full tridiagonal matrix. In this particular case, if $i_1 = 1$ and $i_2 = 3$, then $|D_{i_1} \cap D_{i_2}| = 1$.

Based on the above discussion, it is desirable for the successive elements of the sequence i_r to be elements of $\bigcup_{m=1}^{r-1} D_{i_m}$. The above condition has another positive aspect. Specifically, for a given m , if the indices i_r and i_m are nearest neighbors, it can be expected that $D_{i_r} \cap D_{i_m}$ may potentially contain more elements than the pair $\{i_r, i_m\}$. Evidently, this improves the precision of parameter estimation in the alignment process.

Example 5 (Cont.). Let us investigate two scenarios based on Example 4, considering different choices of the skeleton sequence $J = i_1, i_2, \dots, i_{|J|}$.

In the first scenario, $i_j = j + 1$ so $D_{i_j} = \{i_j - 1, i_j, i_j + 1\}$, for $j = 1, \dots, d - 2$. With this choice of J , for $r > 1$, $\sum_{m=1}^{r-1} |D_{i_m} \cap D_{i_r}| = 2$. Since the neighborhoods $D_{i_1}, \dots, D_{i_{r-2}}$ are disjoint from D_{i_r} , they do not affect parameter estimation. In addition, D_{i_r} shares exactly two neighbors (indices $i_r - 1$ and i_r) with neighborhood $D_{i_{r-1}}$. Consequently, in the alignment process, the parameter a is selected at each step such that the positions of indices $i_r - 1$ and i_r in local configurations $x^{(r-1)}$ and $x^{(r)}$ maintain the same relative ordering. Furthermore, it can be shown that, in practical terms, this alignment process corresponds to adding subsequent indices in a single direction. As a result, the global configuration satisfies the relation $x_1 < x_2 < \dots < x_d$ or $x_1 > x_2 > \dots > x_d$. In either case, the resulting permutation remains optimal.

In contrast, the second scenario highlights the potential consequences of incorrectly estimating the parameter a . Let $i_j = 2j$. With this choice of J , for every $r > 1$, $\sum_{m=1}^{r-1} |D_{i_m} \cap D_{i_r}| = 1$. Specifically, each subsequent neighborhood D_{i_r} is again disjoint from the neighborhoods $D_{i_1}, \dots, D_{i_{r-2}}$ and shares exactly one neighbor (index $i_r - 1$) with the neighborhood $D_{i_{r-1}}$. At each step, the objective function (4.8) has two global minima: one at $a = 1$ and the other at $a = -1$. The parameter b , which controls translation, is determined in the alignment process such that the locations of the shared neighbor ($i_k - 1$) in the local configuration vectors $x^{(k-1)}$ and $x^{(k)}$ overlap. If at any step the procedure erroneously selects the value for a , the direction of adding subsequent elements reverses. Until the next error occurs, elements continue to be added in the wrong direction. Consequently, due to the changes in direction caused by each additional error, the global configuration will exhibit regions affected by “errors”, where relatively distant elements are interspersed. Consequently, the width of Σ under the resulting permutation π may be large.

The last criterion concerns the computational complexity of determining parameters in the alignment process. According to the estimation formula (4.9), it is essential

Algorithm 4.4 Skeleton selection

INPUT: D – A list of d subsets of $\{1, \dots, d\}$ representing neighborhoods
 $z = 1; t = 0;$
 $J[z] = \text{random}(1, \dots, d); \{\text{Initiation of the skeleton, an integer at random}\}$
 $L[[t]] = \{J[z]\}; \{\text{Initiation of the list of outskirts}\}$
 $N[[t]] = \{J[z]\}; \{\text{Initiation of the list of neighborhoods}\}$
while $L[[t]] \neq \emptyset$ **do**
 $t = t + 1;$
 $L[[t]] = \bigcup_{j \in L[[t-1]]} D[[j]] \setminus N[[t-1]]; \{\text{The } t\text{-th order outskirts of } J[z]\}$
 $N[[t]] = N[[t-1]] \cup L[[t]]; \{\text{The } t\text{-th order neighborhood of } J[z]\}$
end while
for $r = 2$ to t **do**
 $X = L[[r]];$
 while $X \neq \emptyset$ **do**
 $j = \text{random}(X); \{\text{random pick from the non-empty outskirts}\}$
 $z = z + 1;$
 $W = D[[j]] \cap L[[r-1]];$
 $J[z] = \text{random} \left(\underset{a \in W}{\text{argmax}} |D_a| \right);$
 $X = X \setminus D[[J[z]]];$
 end while
end for
 RETURN: J – The skeleton of rows.

to identify which sets D_{i_m} intersects non-trivially with D_{i_r} . Since each set D_j intersects non-trivially only with sets D_m for which $m \in \bigcup_{i \in D_j} D_i$, we can construct the sequence i_r to leverage this relationship. This approach reduces the number of intersections evaluated in (4.9).

To present the main algorithm, we define the t -order neighborhoods $D_i(t)$ and their outskirts $L_i(t)$ recurrently. Initially, $D_i(0) = \{i\}$ and $L_i(0) = \{i\}$, and for $t \geq 1$

$$\begin{aligned}
 L_i(t) &= \bigcup_{j \in L_i(t-1)} D_j \setminus D_i(t-1), \\
 D_i(t) &= D_i(t-1) \cup L_i(t).
 \end{aligned}$$

Since $D_i(1) \subseteq D_i(2) \subseteq \dots \subseteq D_i(t)$ for any t , the sets $L_i(1) = D_i(1) \setminus D_i(0)$, $L_i(s) = D_i(s) \setminus D_i(s-1)$, for $s \geq 2$, are disjoint. We refer to them as the outskirts of order s associated with row i . For $j \in L_i(t)$, we have

$$(4.11) \quad D_j \subseteq L_i(t-1) \cup L_i(t) \cup L_i(t+1).$$

In consequence, if $j \in L_i(t)$, $m \in L_i(t+s)$ and $s \geq 3$, then $D_j \cap D_m = \emptyset$.

Algorithm 4.4 schematically presents the selection of J . During the selection process, we track which set $L_i(t)$ each element belongs to. By utilizing (4.11), the

number of sets considered in formula (4.9) can be efficiently reduced. More specifically, for a fixed r , if we partition the index set $I = \{i_1, \dots, i_{r-1}\}$ into disjoint subsets $I(t) = I \cap L_j(t)$ and assume that $i_r \in L_j(s)$, then in formula (4.9), we only consider indices within the set $I(s-2) \cup I(s-1) \cup I(s) \cup I(s+1) \cup I(s+2)$ instead of the entire set I . For large r , this can significantly reduce the computational complexity. Additionally, for any u where $L_i(u) \neq \emptyset = L_i(u+1)$, the sequence of the sets $L_i(1), L_i(2), \dots, L_i(u)$ is a partition of $\{1, \dots, d\}$. This guarantees the completeness of the skeleton. Reducing the size of J improves computational efficiency. While our method attempts to limit its size, our priority is ensuring accurate parameter estimation during the alignment process. Consequently, the algorithm is primarily designed with this objective in mind.

In the algorithm described above, randomness occurs in three places: in the selection of the initial index i_1 , in the choice of an element j from the set X , and in the selection of its neighbor i_z . A key aspect in this context is obtaining a sequence i_r 's with the property that $|D_{i_r}| \approx 2l_{i_r}^{(\pi)} + 1$ (for optimal π), as this yields small upper-bound for the approximation of distance matrices. Currently, no comparative criterion exists to determine optimal indices, and therefore, we select a random index with as large as possible neighborhood in a set W (see Alg.(4.4)), as this may contribute to a more accurate estimation of the parameter a (particularly when the neighborhood overlaps significantly with those of previously selected indices). Additionally, such a choice may facilitate a reduction in the number of indices in the set J , since fewer indices might be required to achieve full coverage of the entire index set.

5. Simulation based performance. The code required to reproduce the simulations presented in this section is publicly available². We evaluate the performance of the packing algorithm on simulated permuted band, block-tridiagonal, and dyadic matrices. The main focus is on the permuted band and block-tridiagonal matrices. Block-tridiagonal matrices, defined at the end of Section 3, include $d \times d$ band matrices with a narrow half-bandwidth as an important subclass. The half-bandwidth of a matrix Σ is given by $\lambda = \|\mathbf{l}\|_\infty = \max\{l_i : i = 1, \dots, d\}$, where $\mathbf{l} = (l_i)_{i=1}^d$ is defined as in Definition 4.1 under the identity permutation. Although our algorithm is primarily designed for permuted band and block-tridiagonal matrices, simulations indicate that it also has the potential to effectively detect dyadic structures. This ability arises from the algorithm's tendency to pack nonzero terms densely around the diagonal, thereby revealing patterns that emerge from variations in row-wise widths of the packed matrix.

Before presenting the simulation results for different classes of matrices, we first examine the role of higher-order neighborhoods in the algorithm.

Before presenting the simulation results for different classes of matrices, we examine the role of higher-order neighborhoods in the algorithm. As in the previous section and without loss of generality, we assume that Σ is a 0 – 1 matrix. Furthermore, let $\Sigma(t)$ denote the 0 – 1 matrix representing row connections in t -th order neighborhoods, more precisely, $\Sigma_{ij}(t) = 1$ iff $j \in D_i(t)$. For a permuted full band matrix Σ , we define $\tilde{\Pi}(\Sigma)$ as the set of permutations π such that $\pi^\top \Sigma \pi$ is a full band matrix. Recall that $\Pi(\Sigma)$ is the set of optimal permutations, i.e., those that minimize half-width. Intuitively, for a permuted full-band matrix Σ , one may expect $\tilde{\Pi}(\Sigma) = \Pi(\Sigma)$. Similarly, since the matrices $\Sigma(k)$ of k -th order neighbors also form permuted full-band matrices, one may expect $\tilde{\Pi}(\Sigma(k)) = \Pi(\Sigma(k))$. These facts are

²See Github repository: <https://github.com/MK8404/Packing-Algorithm>

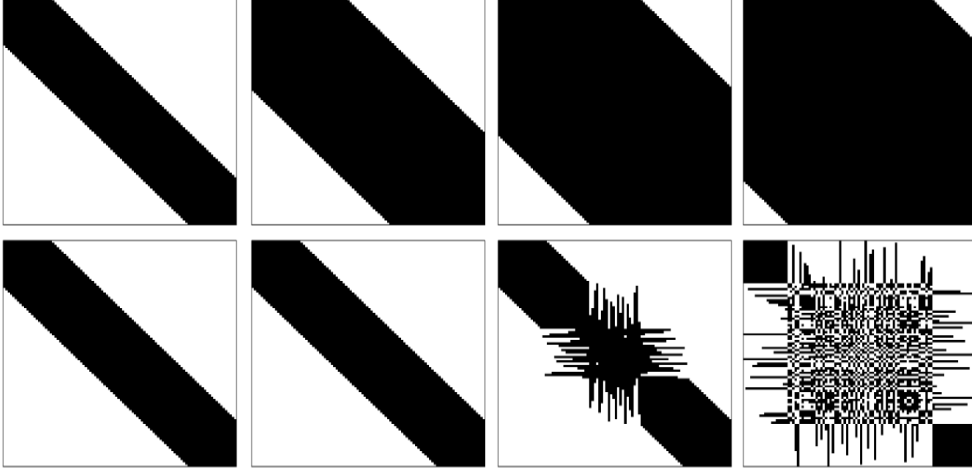


FIG. 1. Effect of increasing the neighborhood size for finding the optimal permutation for the matrix Σ . The first row shows $\Sigma(s)$, $s = 1, 2, 3, 4$ for a 100×100 full band matrix Σ with a half-bandwidth $\lambda = 20$. The second row shows the matrices recovered by applying the permutations obtained from the packing algorithm to the randomly permuted matrices in the first row.

formally established in the next two theorems, with proofs provided in Appendix B.

THEOREM 5.1. *Let Σ be a $d \times d$ permuted full band matrix, then $\tilde{\Pi}(\Sigma) \subseteq \Pi(\Sigma)$.*

Remark 5.2. A stronger result holds that, if $\lfloor \frac{d}{\lambda} \rfloor > \lfloor \frac{d-1}{\lambda+1} \rfloor$, then $\tilde{\Pi}(\Sigma) = \Pi(\Sigma)$. The inequality $\lfloor \frac{d}{\lambda} \rfloor > \lfloor \frac{d-1}{\lambda+1} \rfloor$ is always satisfied when $\lambda^2 \leq d$. On the other hand, when $\lambda^2 > d$, it may or may not hold. Simulations suggest that the inequality is primarily a technical condition and that, regardless of whether it holds, the equality $\tilde{\Pi}(\Sigma) = \Pi(\Sigma)$ remains valid. However, when $\lfloor \frac{d}{\lambda} \rfloor = \lfloor \frac{d-1}{\lambda+1} \rfloor$, the result is still a conjecture.

THEOREM 5.3. *If a $d \times d$ matrix Σ is such that for a permutation $\tilde{\pi}$, $\tilde{\pi}^\top \Sigma \tilde{\pi}$ is a full band matrix with the half-bandwidth $\lambda \geq 1$, then the following conditions hold*

- i) for $t \geq 1$, $\tilde{\pi}^\top \Sigma(t) \tilde{\pi}$ is a full band matrix with a half-bandwidth $t\lambda$,
- ii) if $2\lambda t + 1 \leq d$, then $\tilde{\Pi}(\Sigma(t)) = \{\tilde{\pi}, \rho \circ \tilde{\pi}\}$, where $\rho(s) = d + 1 - s$ for $s = 1, \dots, d$,
- iii) if $2\lambda t + 1 > d$, then $|\tilde{\Pi}(\Sigma(t))| = 2 \cdot (2\lambda t + 2 - d)!$ and $\tilde{\Pi}(\Sigma(t)) \subset \tilde{\Pi}(\Sigma(t+1))$.

Theorems 5.1 and 5.3 offer a characterization of optimal permutations for permuted full band matrices. We can determine the optimal permutations directly, since finding a permutation π such that $\pi^\top \Sigma \pi$ is a full band matrix can be done constructively. Simulations show that, given that $2\lambda + 1 \leq d$, our packing algorithm always returns an optimal permutation for a class of permuted full-band matrices, as displayed in the first two columns of Figure 1. However, in the remaining two columns, where $2\lambda s + 1 > d$, applying the algorithm to $\Sigma(s)$ fails to retrieve the optimal permutation for Σ , which agrees with condition iii) of Theorem 5.3. This illustrates that while increasing the order of neighborhoods improves the approximation to permuted full band matrices, it has limitations, as discussed in the following section.

5.1. Permuted band matrices. In Theorem 5.3, we assumed that Σ is a permuted full band matrix. However, such matrices are not often encountered in practice, as real-world sparse matrices typically do not fully fill up the band. Nonetheless, our simulations show that the packing algorithm remains effective as long as the matrix

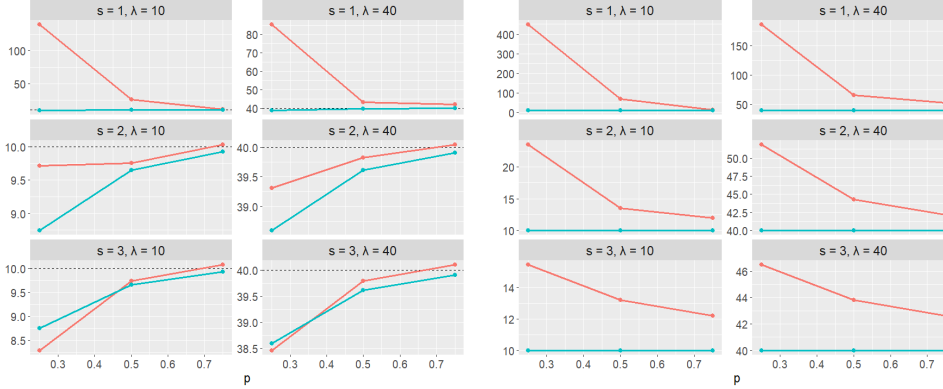


FIG. 2. The average half-width $\|\mathbf{l}^{(\pi)}\|_1/d$ (the first two columns) and $\|\mathbf{l}^{(\pi)}\|_\infty$ (the remaining two columns) as a function of p . Rows correspond to different values of parameter $s \in \{1, 2, 3\}$ and columns correspond to different values of the parameter $\lambda \in \{10, 40\}$. The blue lines in each plot represent values calculated over the initial (before permutation) matrices, while the red lines correspond to averages calculated over the final matrices obtained by the packing algorithm.

retains sufficient density within the band. This effectiveness can be attributed to two main factors. The first is the sparsity of the sets $\{\pi(k) : k \in D_i\}$ within $\pi(i) + C(l_i^{(\pi)})$. According to Remark 4.8, the sparser sets $\{\pi(k) : k \in D_i\}$ are within $\pi(i) + C(l_i^{(\pi)})$, the larger the upper bounds in Theorem 4.5 tend to become, leading to poorer approximations of \mathbf{G}_π by \mathbf{A}_Σ . The second factor is the impact of the cardinality of sets D_i on the classical MDS method. Smaller sets D_i result in smaller distance matrices used for determining local configurations, which can degrade the quality and stability of the resulting configuration.

For permuted band matrices, applying the algorithm to higher-order neighborhoods often results in more accurate approximations of the optimal permutation. This is because considering higher-order neighborhoods simultaneously mitigates the two factors previously identified as reducing the quality of the estimation of the optimal permutation. On one hand, considering higher-order neighborhoods ($t > 1$) naturally increases the number of neighbors for which distances can be computed. Thus, the condition $D_i \cap D_j \neq \emptyset$ can be relaxed to $D_i(t) \cap D_j(t) \neq \emptyset$. Moreover, for an optimal permutation π , the matrices $\pi^\top \Sigma(s) \pi$ on average have a higher percentage of non-zero elements within the band compared to $\pi^\top \Sigma \pi$. Consequently, they more closely follow the efficiency of the algorithm for permuted full-band matrices.

In the simulations, we considered 1000×1000 band matrices obtained from the full band matrices having the half-band width $\lambda \in \{10, 40\}$ by randomly and independently setting some elements within the band to zero with probability $1 - p$, $p \in \{0.25, 0.5, 0.75\}$. The resulting 0-1 band matrix was ensured to be symmetric and the neighborhoods of order $s \in \{1, 2, 3\}$ were considered. Finally, the rows and columns of each generated band matrix were randomly permuted. We applied our packing algorithm and used the resulting permutation to recover the initial band matrix. We then computed and compared the half-width and half-bandwidth of the initial and final matrices to assess the packing quality. For each combination of (λ, p, s) , the experiment was repeated 100 times.

The first two columns of Figure 2 display the results of simulations for half-width divided by d as a function of parameter p . The blue curves describe the functional relationship between the half-width and the parameter p for the initial matrices. The

plots in the second and third rows show that the blue curves have similar shapes across columns. Thus, we use the blue curves as a reference for analyzing the red curves, which correspond to the results from the packing algorithm. The functional relationship described by the blue curves is quite intuitive, as the initial matrices are created by randomly zeroing a portion of elements within the band. Therefore, the more elements zeroed out, the smaller the half-width should be, which is reflected in the behavior of the blue curves.

We now focus on the red curves associated with the final results. For $s = 1$, the red curves represent decreasing functions. Specifically, for the sparsest matrices ($p = 0.25$), the results significantly deviate from the optimal solution. However, as p increases, the solutions become increasingly accurate. This observation aligns with previous findings, as it indicates that when the set $\{\pi(k) : k \in D_i\}$ within $\pi(i) + C(l_i^{(\pi)})$ becomes denser, the approximation of the true distances between rows becomes more accurate, leading to a better approximation of the optimal permutation. As seen in the second and third rows, incorporating higher-order neighborhoods further improves the final results. The blue and red curves are relatively close to each other. Notably, in the third row for $p = 0.25$, the packing algorithm (on average) was able to find permutations resulting in a smaller average half-width than those of the initial matrices. At first glance, one might expect that the initial matrix is exactly the optimal solution. However, when $p = 0.25$, the initial matrix is formed by removing approximately 75% of the nonzero elements from the full band matrix, which paradoxically leads to a structure that allows for even denser packing around the diagonal. This highlights the strong performance of the packing algorithm in minimizing half-width.

Finally, we note that band matrices are closely related to the bandwidth minimization problem, which aims to find a permutation π that minimizes the half-bandwidth $\|\mathbf{L}^{(\pi)}\|_\infty$ of $\boldsymbol{\pi}^\top \boldsymbol{\Sigma} \boldsymbol{\pi}$. Interestingly, although designed for a different purpose, our packing algorithm provides highly effective solutions to this problem in many cases, as illustrated in the third and fourth columns of Figure 2. The blue curves are constant functions with values equal to the parameter λ , as expected. In theory, removing non-zero elements could occasionally reduce the half-bandwidth, but this is highly unlikely in considered cases.

It is easy to see that $\boldsymbol{\Sigma}(s)$, which now also depends on p , λ , and d , must be a band matrix with a half-bandwidth no greater than $s \cdot \lambda$. Therefore, we can compare *the level of (band) filling* for different parameter combinations by determining the proportion of nonzero elements within the band for each matrix

$$F(s) = \frac{\sum_{i=1}^d |\{j : \boldsymbol{\Sigma}_{ij}(s) \neq 0\}|}{\sum_{i=1}^d |\{j : |i - j| \leq s\lambda\}|}.$$

This statistic for $\boldsymbol{\Sigma}(s)$ measures the proportion of elements in sets $\pi(k) : k \in D_i(s)$ that belong to sets $\pi(i) + C(l_i^{(\pi)})$. As mentioned earlier, a higher level of filling leads to a better approximation of actual distances and, consequently, improved properties of the final permutation.

Figure 3 (left panel) presents the level of band filling as a function of p for various parameter combinations. The solid line for $s = 1$ is linear, which follows naturally from the construction of the initial matrix. The slightly higher function values relative to p stem from the fact that the diagonal elements were excluded from the random zeroing process. In contrast, the dashed lines ($s \in \{2, 3\}$) exhibit noticeably higher levels of filling. This translates into greater effectiveness of the packing algorithm, as a higher level of filling results in a better approximation of the optimal permutation.

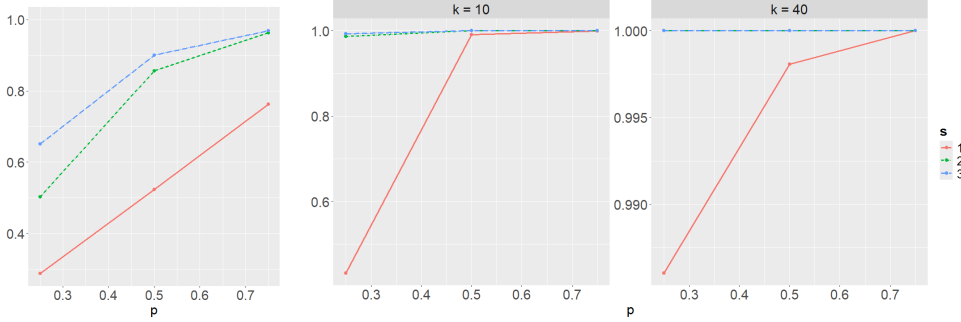


FIG. 3. The first plot presents the average $F(s)$ obtained for band matrices, $\lambda = 10$. The second and the third plots present the average proportion of nonzero elements within the tridiagonal block structure returned by the packing algorithm applied to randomly permuted tridiagonal matrices with widths $k = 10$ and $k = 40$. The graphs are functions of the level of filling p for $s \in \{1, 2, 3\}$.

The simulations indicate that the level of filling F is a non-decreasing function of the parameter s with the increase being particularly pronounced when $p = 0.25$. However, once F exceeds a certain threshold, its further increase does not necessarily lead to a significant improvement in the properties of the returned permutation. This effect is especially evident in the second and third rows for $p \geq 0.5$, where the differences between the red and blue curves become marginal.

The above observation is crucial for two reasons. First, incorporating higher-order neighborhoods inherently increases the computational complexity of the algorithm. Second, according to Theorem 5.3, when the parameter s is sufficiently large ($2s\lambda^{(\pi)} + 1 > d$), the problems of determining the optimal permutation for the full band matrix Σ and for $\Sigma(s)$ are no longer equivalent (specifically, $\Pi(\Sigma) \subsetneq \Pi(\Sigma(s))$). Consequently, the algorithm fails to return accurate solutions, as illustrated in Figure 1.

5.2. Block tridiagonal matrices. For block tridiagonal matrices, the packing algorithm performs very similarly to its behavior on band matrices. The main difference is that it also retrieves the block structure by packing nonzero elements efficiently, which is an important result of using $\|\cdot\|_1$ norm for the optimality criterion.

The simulation setup is the same as before, except the dimension $d = k(2^N - 1)$ is chosen to match complete dyadic matrices. We take $N = 4$ (height) and $k \in \{10, 40\}$ (breadth/block size). The results of the analysis are presented in Figure 4. This figure is organized similarly to those depicting the same statistic in previous sections, except the breadth k replaces the half-bandwidth λ . The plots indicate that the algorithm produces results comparable to those obtained for band matrices. When the parameter $p \geq 0.5$, the results are close to optimal regardless of the values of parameters s and k .

For $p = 0.25$ (the sparsest case), when $s = 1$, the algorithm yields weaker results for $k = 10$. Notably, for $p = 0.5$ and $p = 0.75$ ($s = 1$), the algorithm, on average, produces matrices with better properties than the initial matrix. Interestingly, for $k = 40$ it outperforms the results obtained using higher-order neighborhoods that are presented in the second and third rows. These findings further emphasize the strong performance of the packing algorithm and demonstrate that higher-order neighborhoods are not always necessary for achieving good approximations of the optimal permutation. Nevertheless, as seen in the second and third rows, incorporating higher-order neighborhoods significantly enhances the approximation of the optimal

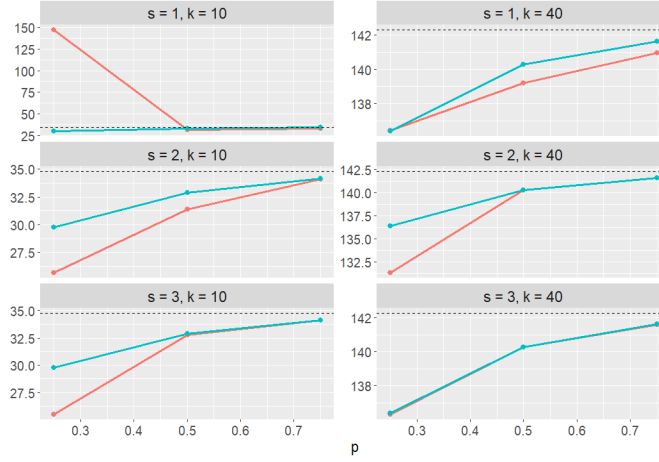


FIG. 4. The average half-width $\|l^{(\pi)}\|_1/d$ for permuted tridiagonal matrices shown as a function of p with $N = 4$. Rows correspond to $s \in \{1, 2, 3\}$, and columns to $k \in \{10, 40\}$. The blue lines represent values calculated over the initial (not permuted) matrices, while the red lines correspond to averages calculated over the final matrices obtained by the packing algorithm.

permutation. Notably, the algorithm is capable of identifying a better permutation for sparse matrices than simply returning the initial matrix. The underlying causes of this behavior appear to be similar to those observed for band matrices.

From the perspective of the dyadic algorithm, it is crucial that the packing algorithm returns a matrix with a tridiagonal block structure. Figure 3 (middle and right panels) presents, on a scale from 0 to 1, the average proportion of nonzero elements within the tridiagonal block structure of the original full tridiagonal matrix. It is evident that when higher-order neighborhoods are utilized (second and third rows), nearly all observations remain within the structure. Only for $p = 0.25$ does a small fraction of elements fall outside, but this proportion does not exceed 3%. For the first row, the results remain strong when $p \geq 0.5$; however, for the sparsest matrices ($p = 0.25$), the algorithm produces comparatively weaker solutions. This outcome is expected, as a similar trend was observed in the half-width statistic, which also indicated reduced solution quality for this specific parameter configuration.

5.3. Dyadic matrices. For dyadic matrices, the direct application of the packing algorithm is unable to recover the original structure. However, the algorithm can be applied iteratively since a dyadic matrix, formally, is a block-diagonal matrix with sparsely filled “nonzero” blocks. To illustrate this approach, let us first consider banded dyadic matrices generated by an element-wise multiplication ($\mathbf{A}_{ij} = \mathbf{B}_{ij}\mathbf{C}_{ij}$ for every pair of indices i, j) of a full band matrix \mathbf{B} with a half-bandwidth λ by a dyadic matrix \mathbf{C} . See the upper-left panel of Figure 5.

The first two columns of Figure 5 display the effect of applying the packing algorithm to the first and second powers of the banded dyadic matrix. In the first row, we present a banded dyadic matrix, $N = 5, k = 10, p = 0.5, \lambda = 60$, along with its second power. These matrices are structurally similar to those considered in the previous section. In particular, the second matrix closely resembles a full block - tridiagonal matrix, a class of matrices for which the effectiveness of the packing algorithm was demonstrated in previous sections. Therefore, it is unsurprising that the packing algorithm in this scenario successfully recovered the outermost block

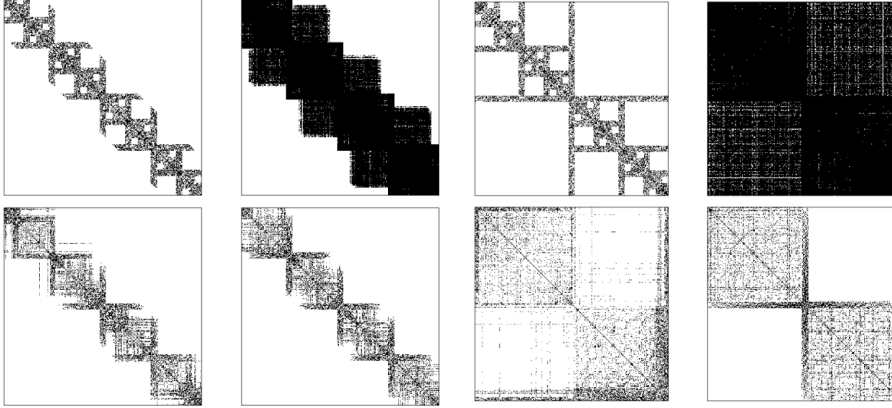


FIG. 5. The performance of the packing algorithm for a banded dyadic matrix, $\lambda = 60$, (the first two columns) and a dyadic matrix (the two remaining columns), ($N = 5, k = 10, p = 0.5$). The top graphs display the original (non-permuted) matrices along with their second power. The bottom graphs show the matrices recovered by the algorithm.

structure of the banded dyadic matrix. The results are shown in the second row, where the first and second images represent the resulting matrices after applying the packing algorithm to the distance matrices $\mathbf{A}(1)$ and $\mathbf{A}(2)$, respectively. However, the algorithm completely fails to recover the internal structure of the banded dyadic matrix. This is expected, as the algorithm's primary objective is to minimize the half-width of the matrix and, in this case, the internal structure does not influence the relevant statistics.

The algorithm's success with banded dyadic matrices is clearly linked to their structural similarity to block-tridiagonal matrices. However, the packing algorithm exhibits notable resilience to deviations from this structural form. The third and fourth columns in Figure 5 illustrate the algorithm's performance for a dyadic matrix in a similar context. Applying the algorithm directly to a dyadic matrix results in a matrix with a considerably large half-width, producing a solution that is far from optimal. However, certain patterns emerge, revealing groups of indices with stronger interconnections.

In contrast, analyzing the second power of the dyadic matrix reveals two distinct phenomena. Firstly, the matrix becomes almost fully populated with nonzero elements, yet these elements lack a clear block structure. Secondly, a block-like pattern emerges, where blocks closer to the diagonal exhibit a denser concentration of nonzero elements compared to those further away. These results suggest that the block-like structure observed in the squared dyadic matrix is sufficient to reconstruct the outermost dyadic structure with reasonable accuracy. This demonstrates the algorithm's remarkable robustness in handling deviations from ideal structural properties while still capturing essential organizational patterns.

The ability of the algorithm to identify the outermost structure of a (banded) dyadic matrix lays the foundation for an iterative approach to approximate the complete reconstruction of the original dyadic structure. The method involves iteratively applying the packing algorithm to extract the “main cross” of the matrix at each step, see Figure 6. After identifying the main cross, the index set is divided into three distinct subsets:

1. indices associated with the “main cross” (green cross)

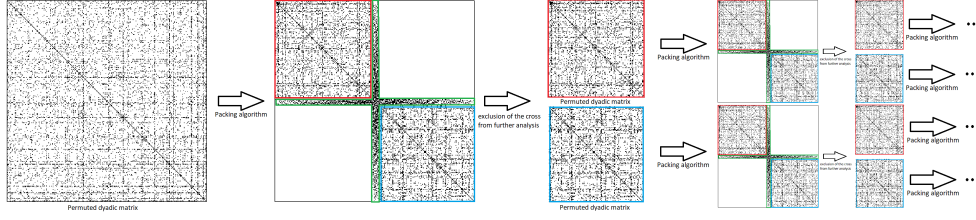


FIG. 6. Iteratively applying the packing algorithm to determine the complete dyadic structure

2. indices “to the left” of the cross (red square)
3. indices “to the right” of the cross (blue square)

Notably, the submatrices associated with the left and right index subsets retain the (banded) dyadic structure. This allows the packing algorithm to be recursively applied to these submatrices to identify their respective “main crosses”, continuing the iterative process until the structure of the entire matrix is retrieved.

6. Conclusions. The paper proposes an efficient approach for the inversion and factorization of sparse matrices structured in a dyadic form. We introduce a new packing algorithm based on the l_1 norm and numerically investigate its properties. The algorithm primarily targets band matrices, which constitute the special case of dyadic matrices. However, it also successfully retrieves block-tridiagonal matrices, enabling an iterative method for packing matrices into a dyadic form. We also show that for band matrices, the packing algorithm identifies permutations that offer reasonable solutions to the bandwidth minimization problem. This classical numerical problem is tangential to the primary focus of our study, but our simulations suggest that the packing algorithm presents a novel and promising approach. The efficiency of many algorithms in this field often relies on the assumption that the initial ordering of the rows and columns in the matrix is sufficiently close to the optimal arrangement. In this context, the solutions provided by our packing algorithm could serve as a good starting point for other procedures. Further investigation is needed to explore this potential.

The first matrix represents a regular and completely dyadic matrix with the red stars indicating locations of possibly nonzero terms, the case of $N = 4$ and $k = 3$:

[illegible]

The next matrix represents an irregular and non-complete dyadic matrix obtained from the original by removing nine columns and corresponding rows

The embedding of the previous irregular and incomplete dyadic matrix to the regular and complete one is obtained by placing in the missing fields the identity matrix as seen in the following

B.1. Proofs of Section 3.

Justification of Algorithm 3.1. Let $\mathbf{P}_1 = \mathbf{P}$, where \mathbf{P} is obtained in the first step of the algorithm before the for-loop and \mathbf{P}_l are \mathbf{P} matrices obtained within the for-loop, $l = 2, \dots, N$. We will argue that \mathbf{P}_l orthonormalizes $\tilde{\mathbf{F}}_l = [\mathbf{F}_1 \dots \mathbf{F}_l]$. The proof goes through the induction and it is obvious that \mathbf{P}_1 orthonormalizes $\tilde{\mathbf{F}}_1$ by the definition of $\mathbf{G}_1(\cdot)$. Assume that for $l \geq 2$, \mathbf{P}_{l-1} orthonormalizes $\tilde{\mathbf{F}}_{l-1} = [\mathbf{F}_1 \dots \mathbf{F}_{l-1}]$. Observe that

$$\begin{aligned} \tilde{\mathbf{F}}_l &= [\tilde{\mathbf{F}}_{l-1} \quad \mathbf{F}_l] \begin{bmatrix} \mathbf{P}_{l-1} & -\mathbf{A}\mathbf{G} \\ \mathbf{0} & \mathbf{G} \end{bmatrix} \\ &= [\tilde{\mathbf{F}}_{l-1}\mathbf{P}_{l-1} \quad (\mathbf{F}_l - \tilde{\mathbf{F}}_{l-1}\mathbf{A}) \mathbf{G}]. \end{aligned}$$

Clearly, by the induction, $\tilde{\mathbf{F}}_{l-1}\mathbf{P}_{l-1}$ is made of the orthonormalized vectors so that

$$\mathbf{P}_{l-1}^\top \tilde{\mathbf{F}}_{l-1}^\top \tilde{\mathbf{F}}_{l-1} \mathbf{P}_{l-1} = \mathbf{I}.$$

Consequently, it is enough to show that, firstly, $\tilde{\mathbf{F}}_{l-1}\mathbf{P}_{l-1} \perp (\mathbf{F}_l - \tilde{\mathbf{F}}_{l-1}\mathbf{A})$ and, secondly, that \mathbf{G} orthonormalizes $(\mathbf{F}_l - \tilde{\mathbf{F}}_{l-1}\mathbf{A})$.

The first part follows from

$$\begin{aligned} \mathbf{P}_{l-1}^\top \tilde{\mathbf{F}}_{l-1}^\top (\mathbf{F}_l - \tilde{\mathbf{F}}_{l-1}\mathbf{A}) &= \mathbf{P}_{l-1}^\top \tilde{\mathbf{F}}_{l-1}^\top \mathbf{F}_l - \mathbf{P}_{l-1}^\top \tilde{\mathbf{F}}_{l-1}^\top \tilde{\mathbf{F}}_{l-1} \mathbf{P}_{l-1} \mathbf{P}_{l-1}^\top \begin{bmatrix} \boldsymbol{\Sigma}_{1,l} \\ \vdots \\ \boldsymbol{\Sigma}_{l-1,l} \end{bmatrix} \\ &= \mathbf{P}_{l-1}^\top \begin{bmatrix} \boldsymbol{\Sigma}_{1,l} \\ \vdots \\ \boldsymbol{\Sigma}_{l-1,l} \end{bmatrix} - \mathbf{P}_{l-1}^\top \begin{bmatrix} \boldsymbol{\Sigma}_{1,l} \\ \vdots \\ \boldsymbol{\Sigma}_{l-1,l} \end{bmatrix}. \end{aligned}$$

The second part follows from the fact that

$$\begin{aligned} &(\mathbf{F}_l - \tilde{\mathbf{F}}_{l-1}\mathbf{A})^\top (\mathbf{F}_l - \tilde{\mathbf{F}}_{l-1}\mathbf{A}) \\ &= (\mathbf{F}_l - \tilde{\mathbf{F}}_{l-1}\mathbf{A})^\top \mathbf{F}_l - (\mathbf{F}_l - \tilde{\mathbf{F}}_{l-1}\mathbf{A})^\top \tilde{\mathbf{F}}_{l-1}\mathbf{A} \\ &= \boldsymbol{\Sigma}_{l,l} - \mathbf{A}^\top \tilde{\mathbf{F}}_{l-1}^\top \mathbf{F}_l - (\mathbf{F}_l - \tilde{\mathbf{F}}_{l-1}\mathbf{A})^\top \tilde{\mathbf{F}}_{l-1} \mathbf{P}_{l-1} \mathbf{P}_{l-1}^\top \begin{bmatrix} \boldsymbol{\Sigma}_{1,l} \\ \vdots \\ \boldsymbol{\Sigma}_{l-1,l} \end{bmatrix} \\ &= \boldsymbol{\Sigma}_{l,l} - \mathbf{A}^\top \tilde{\mathbf{F}}_{l-1}^\top \mathbf{F}_l \\ &= \boldsymbol{\Sigma}_{l,l} - [\boldsymbol{\Sigma}_{1,l}^\top, \dots, \boldsymbol{\Sigma}_{l-1,l}^\top] \mathbf{P}_{l-1} \mathbf{P}_{l-1}^\top \begin{bmatrix} \boldsymbol{\Sigma}_{1,l} \\ \vdots \\ \boldsymbol{\Sigma}_{l-1,l} \end{bmatrix} = \tilde{\boldsymbol{\Sigma}}, \end{aligned}$$

and \mathbf{G} orthonormalizes vectors having the gramian equal to $\tilde{\boldsymbol{\Sigma}}$. \square

Proof of Lemma 3.2. First of all, since \mathbf{H} is of shape $k(2^N - 2^{N-l+1}) \times k(2^N - 2^{N-l+1})$, and \mathbf{E} is of shape $k(2^N - 2^{N-l+1}) \times k2^{N-l}$, $\mathbf{H}\mathbf{E}$ will have the same shape as \mathbf{E} .

According to (3.5) and (3.8),

$$(B.1) \quad \mathbf{H}\mathbf{E} = \left(\sum_{s=1}^{2^{N-l+1}} \mathbf{H}_s \right) \left(\sum_{r=1}^{2^{N-l}} \mathbf{E}_r \right)$$

As we know, \mathbf{H}_s is $\mathcal{HD}(l-1)$ in the s -th diagonal $k2^{l-1} \times k2^{l-1}$ block and zero otherwise. On the other hand, \mathbf{E}_r has a block-sparsity pattern corresponding to $\mathcal{ED}(N, l)_t$. Consequently, $\mathbf{H}_s \mathbf{E}_r$ is nonzero only if $s = 2r - 1$ or $s = 2r$. Therefore, (B.1) can be simplified as

$$\mathbf{H}\mathbf{E} = \sum_{r=1}^{2^{N-l}} (\mathbf{H}_{2r-1} + \mathbf{H}_{2r}) \mathbf{E}_r.$$

To compute each summand $(\mathbf{H}_{2r-1} + \mathbf{H}_{2r}) \mathbf{E}_r$, note that the nonzero part of $\mathbf{H}_{2r-1} + \mathbf{H}_{2r}$ is a block-diagonal matrix of size $k(2^l - 2) \times k(2^l - 2)$ with its two diagonal blocks being $\mathcal{HD}(l-1)$. Meanwhile, the nonzero part of matrix \mathbf{E}_r is of size $k(2^l - 2) \times k$ and can be viewed as a 2×1 block matrix whose blocks are each of size $k(2^{l-1} - 1) \times k$. Multiplying these nonzero parts yields a result of size $k(2^l - 2) \times k$, which is exactly the size of the nonzero block in \mathbf{E}_r . Hence, the product $(\mathbf{H}_{2r-1} + \mathbf{H}_{2r}) \mathbf{E}_r$ retains the same block-sparsity pattern as \mathbf{E}_r , and when summed over r , the resulting matrix $\mathbf{H}\mathbf{E}$ exhibits the same block-sparsity pattern as \mathbf{E} , namely $\mathcal{ED}(N, l)$.

In terms of complexity, according to Proposition 3.5, the flops required to calculate each of the summand will be $O((l-1)2^{l-1}k^3)$, and so the total flops required to obtain $\mathbf{H}\mathbf{E}$ will be

$$O((l-1)2^{N-1}k^3) = O(ldk^2).$$

Symmetrically, the proof for $\mathbf{V}\mathbf{E}$ follows an identical logic. $\mathbf{V}\mathbf{E}$ will have the same block-sparsity pattern as \mathbf{E} . Based on Proposition 3.4, the complexity is also $O(ldk^2)$.

For the second part, according to (3.5),

$$\mathbf{E}^\top \mathbf{E} = \left(\sum_{s=1}^{2^{N-l}} \mathbf{E}_s^\top \right) \left(\sum_{r=1}^{2^{N-l}} \mathbf{E}_r \right).$$

From the block-sparsity pattern (3.2), we have that $\mathbf{E}_s^\top \mathbf{E}_r$ is nonzero only if $s = r$. Hence,

$$\mathbf{E}^\top \mathbf{E} = \sum_{s=1}^{2^{N-l}} \mathbf{E}_s^\top \mathbf{E}_s.$$

To obtain each of the summands above is essentially to calculate multiplication of a $k \times k(2^l - 2)$ nonzero matrix with its $k(2^l - 2) \times k$ nonzero counterpart. Such a multiplication will result in a $k \times k$ nonzero matrix, and it costs $O(k^3 2^l)$ flops.

This means that $\mathbf{E}_s^\top \mathbf{E}_s$ will result in a $k2^{N-l} \times k2^{N-l}$ block diagonal matrix with block size $k \times k$ and only the s -th diagonal block of it is nonzero. Therefore, $\mathbf{E}^\top \mathbf{E}$ will be a $k2^{N-l} \times k2^{N-l}$ block diagonal matrix with each of its diagonal block being nonzero. In other words, $\mathbf{E}^\top \mathbf{E} \in \mathcal{D}(N, l)$. The total number of flops required to compute $\mathbf{E}^\top \mathbf{E}$ is

$$O(k^3 2^N) = O(dk^2).$$

Finally, for the last part, we can decompose \mathbf{D} as

$$\mathbf{D} = \sum_{r=1}^{2^{N-l}} \mathbf{D}_r,$$

where \mathbf{D}_r is a block diagonal matrix with $k \times k$ diagonal blocks and only its r -th diagonal block is nonzero. Then we can write

$$\mathbf{E}\mathbf{D} = \left(\sum_{s=1}^{2^{N-l}} \mathbf{E}_s \right) \left(\sum_{r=1}^{2^{N-l}} \mathbf{D}_r \right)$$

Again, referring to (3.7), we know that $\mathbf{E}_s \mathbf{D}_r$ is nonzero only if $s = r$. As a result,

$$\mathbf{E}\mathbf{D} = \sum_{s=1}^{2^{N-l}} \mathbf{E}_s \mathbf{D}_s.$$

To obtain each of the summands above is essentially to calculate multiplication of a $k(2^l - 2) \times k$ nonzero matrix with its $k \times k$ nonzero counterpart, resulting in a $k(2^l - 2) \times k$ nonzero matrix. This means that $\mathbf{E}_s \mathbf{D}_s$ will have the same block-sparsity pattern as \mathbf{E}_s , and hence $\mathbf{E}\mathbf{D}$ will have the same block-sparsity pattern as \mathbf{E} , which is $\mathcal{ED}(N, l)$.

In terms of computational complexity, to calculate each of the summands, one needs $O(k^3 2^l)$ flops, and in total, the number of flops that $\mathbf{E}\mathbf{D}$ requires is

$$O(k^3 2^N) = O(dk^2). \quad \square$$

The proof of Lemma 3.8. Since the refined patterns $\widetilde{\mathcal{ED}}(N, l)$ and $\widetilde{\mathcal{ED}}'(N, l)$ are both subsets of $\mathcal{ED}(N, l)$, it follows from Lemma 3.2 that \mathbf{VHE} inherits the sparsity pattern $\mathcal{ED}(N, l)$. The same as in the proof of Lemma 3.2, we know that

$$\mathbf{H}\mathbf{E} = \sum_{r=1}^{2^{N-l}} (\mathbf{H}_{2^{r-1}} + \mathbf{H}_{2^r}) \mathbf{E}_r,$$

which is essentially the sum of the products of a $k(2^l - 2) \times k(2^l - 2)$ block-diagonal matrix (with its two nonzero diagonal blocks having structure $\mathcal{HD}(l - 1)$) and a $k(2^l - 2) \times k$ submatrix whose block-sparsity pattern is identical to

$$\underbrace{[\mathbf{0}_{k \times k}, \dots, \mathbf{0}_{k \times k}, \mathbf{1}_{k \times k}, \mathbf{1}_{k \times k}, \mathbf{0}_{k \times k}, \dots, \mathbf{0}_{k \times k}]}_{2^{l-1}-2} \underbrace{[\mathbf{0}_{k \times k}, \dots, \mathbf{0}_{k \times k}]}_{2^{l-1}-2}^\top.$$

Therefore, only the rows in the $\mathcal{HD}(l - 1)$ blocks corresponding to the nonzero entries specified by the block-sparsity pattern $\widetilde{\mathcal{ED}}'(N, l)$ are involved in the multiplication, which implies that $\mathbf{H}\mathbf{E} \in \widetilde{\mathcal{ED}}'(N, l)$. In terms of complexity, the number of flops required to evaluate $\mathbf{H}\mathbf{E}$ is

$$O((l - 1)k^3 2^{N-l+1}) = O(k^3 2^N) = O(dk^2).$$

Similarly, the structure of $\mathbf{V} \in \mathcal{IV}(N, l)$ ensures that, in the product \mathbf{VHE} , only the columns corresponding to the nonzero entries in $\widetilde{\mathcal{ED}}'(N, l)$ are involved. The overall computational cost for this multiplication is

$$O\left(k^3 2^{N-l+1} \sum_{r=1}^{l-1} (2^{l-r} - 1)\right) = O(k^3 2^N) = O(dk^2).$$

B.2. Proofs of Section 4.

The proof of Theorem 4.2. Let permutation β orders x_i , i.e. $x_{\beta(1)} < \dots < x_{\beta(d)}$. Assuming that one has the information about $\mathcal{I}(\mathbf{G}_{\mathbf{x}})$, we pick up one of the two indices of the endpoints, say $\alpha(1) = j_e^1$, and set $y_1 = 0$. There are two possibilities, either $\alpha(1) = \beta(1)$ or $\alpha(1) = \beta(d)$. Let us first consider the first case.

Furthermore, there is only one $i \in \{1, \dots, d\} \setminus \{\alpha(1)\}$ such that $\alpha(1) \in \{j_i^1, j_i^2\}$. We define $\alpha(2) = i$ and $y_2 = \rho$, where ρ is the one from $\{\rho_i^1, \rho_i^2\}$ that corresponds to $\alpha(1)$. We observe that $\alpha(2) = \beta(2)$ and

$$|y_2 - y_1| = y_2 - y_1 = x_{\alpha(2)} - x_{\alpha(1)} = |x_{\alpha(2)} - x_{\alpha(1)}|.$$

Then we define recurrently $\alpha(k)$, and y_k , for $k = 3, \dots, d-1$. Given $\alpha(1), \dots, \alpha(k-1)$ and $y_1 < \dots < y_{k-1}$, such that

$$(B.2) \quad \begin{aligned} \alpha(l) &= \beta(l), \quad l = 1, \dots, k-1, \\ x_{\alpha(l+1)} - x_{\alpha(l)} &= y_{l+1} - y_l, \quad l = 1, \dots, k-2, \end{aligned}$$

we define $\alpha(k)$ as the only $i \notin \{\alpha(1), \dots, \alpha(k-1)\}$ such that $\alpha(k-1) \in \{j_i^1, j_i^2\}$. Furthermore, we define $y_k = y_{k-1} + \rho$, where ρ is the one from $\{\rho_i^1, \rho_i^2\}$ that corresponds to $\alpha(k-1)$. It is clear that $x_{\alpha(k)}$ corresponds to the in-between point corresponding to $\{(j_i^1, \rho_i^1), (j_i^2, \rho_i^2)\}$ and thus $\alpha(k) = \beta(k)$. This way we assure that (B.2) is also satisfied for $l = k-1$. Moreover, $\alpha(d)$ is the last missing index not added yet to the sequence α and $y_d = y_{d-1} + \rho$, where ρ is the one from $\{\rho_{\alpha(d-1)}^1, \rho_{\alpha(d-1)}^2\}$ that corresponds to $\alpha(d)$. It is straightforward to verify that the (B.2) remains satisfied for $k = d$ as well.

Let redefine \mathbf{y} as $y_{\alpha^{-1}(k)}$, $k = 1, \dots, d$, which assures by (B.2) that

$$x_{\alpha(l+1)} - x_{\alpha(l)} = y_{\alpha(l+1)} - y_{\alpha(l)},$$

and thus for $s = x_{\alpha(1)}$

$$\mathbf{x} = s + \mathbf{y}.$$

As a direct implication of the above relation, we obtain $\mathbf{G}_{\mathbf{x}} = \mathbf{G}_{\mathbf{y}}$.

To argue for the case when $\alpha(1) = \beta(d)$, consider $\tilde{\mathbf{x}} = -\mathbf{x}$ for which $\alpha(1) = \tilde{\beta}(1)$ and $\mathbf{G}_{\mathbf{x}} = \mathbf{G}_{\tilde{\mathbf{x}}}$. By the previous argument we construct \mathbf{y} such that $\tilde{\mathbf{x}} = -\mathbf{x} = \tilde{s} + \mathbf{y}$, which means that $\mathbf{x} = -\tilde{s} - \mathbf{y}$. \square

The next part of this section is devoted to the proof of Theorem 4.5, which requires some auxiliary results.

LEMMA B.1. *Under the assumptions of Theorem 4.5, it holds*

$$|\pi(i) - \pi(j)| = \frac{1}{2} \left| \left(\pi(i) + C(l_i^{(\pi)}) \right) \triangle \left(\pi(j) + C(l_j^{(\pi)}) \right) \right|,$$

where $C(t) = \{-t, \dots, -1, 0, 1, \dots, t\}$.

Proof. Without losing generality, one can assume that $\pi(i) < \pi(j)$. The assumed inequalities

$$|l_i^{(\pi)} - l_j^{(\pi)}| \leq |\pi(i) - \pi(j)| \leq l_i^{(\pi)} + l_j^{(\pi)}$$

yield

$$(B.3) \quad \begin{aligned} \pi(i) - l_i^{(\pi)} &\leq \pi(j) - l_j^{(\pi)}, \\ \pi(i) + l_i^{(\pi)} &\leq \pi(j) + l_j^{(\pi)}, \\ \pi(i) + l_i^{(\pi)} &\geq \pi(j) - l_j^{(\pi)}. \end{aligned}$$

The first inequality indicates that the smallest element in the set $\pi(i) + C(l_i^{(\pi)})$ provides a lower bound for the set $\pi(j) + C(l_j^{(\pi)})$. Similarly, the second inequality implies that the largest element in the set $\pi(j) + C(l_j^{(\pi)})$ provides an upper bound for the set $\pi(i) + C(l_i^{(\pi)})$. The third inequality signifies that the intersection of the two sets is non-empty. In consequence,

$$\begin{aligned} & \frac{1}{2} \left| \left(\pi(i) + C(l_i^{(\pi)}) \right) \triangle \left(\pi(j) + C(l_j^{(\pi)}) \right) \right| \\ &= \frac{1}{2} \left| \left(\pi(i) + C(l_i^{(\pi)}) \right) \setminus \left(\pi(j) + C(l_j^{(\pi)}) \right) \right| + \frac{1}{2} \left| \left(\pi(j) + C(l_j^{(\pi)}) \right) \setminus \left(\pi(i) + C(l_i^{(\pi)}) \right) \right| \\ &= \frac{1}{2} \left[(\pi(j) - l_j^{(\pi)}) - (\pi(i) - l_i^{(\pi)}) \right] + \frac{1}{2} \left[(\pi(j) + l_j^{(\pi)}) - (\pi(i) + l_i^{(\pi)}) \right] \\ &= \pi(j) - \pi(i). \end{aligned}$$

The equality between the second and third line is coming from the fact that $\pi(k) + C(l_k^{(\pi)})$, for $k = i, j$, are sets of consecutive integer numbers and inequalities (B.3). This ends the proof of the lemma. \square

LEMMA B.2. *Suppose Z_1, Z_2, A_1, A_2 are subsets of $(1, \dots, d)$. For any permutation π of $(1, \dots, d)$, if $\pi(Z_1) \subseteq A_1$ and $\pi(Z_2) \subseteq A_2$, then*

$$|Z_1 \cap Z_2| \leq |A_1 \cap A_2| \leq |Z_1 \cap Z_2| + |A_1| - |Z_1| + |A_2| - |Z_2|.$$

Proof. From the assumption

$$|\pi(Z_1) \cap \pi(Z_2)| \leq |A_1 \cap A_2|.$$

On the other hand

$$\pi(Z_1) \cap \pi(Z_2) = \{\pi(m) : m \in Z_1\} \cap \{\pi(m) : m \in Z_2\} = \{\pi(m) : m \in Z_1 \cap Z_2\}.$$

Hence the cardinality of sets $\pi(Z_1) \cap \pi(Z_2)$ and $Z_1 \cap Z_2$ is the same, which ends the proof of the first inequality in the lemma.

To prove the second inequality, we note that if $B_1 \subseteq \bar{B}_1$ and $B_2 \subseteq \bar{B}_2$, then

$$\bar{B}_1 \cap \bar{B}_2 \subseteq (B_1 \cap B_2) \cup (\bar{B}_1 \setminus B_1) \cup (\bar{B}_2 \setminus B_2),$$

and in consequence

$$|\bar{B}_1 \cap \bar{B}_2| \leq |B_1 \cap B_2| + |\bar{B}_1 \setminus B_1| + |\bar{B}_2 \setminus B_2| = |B_1 \cap B_2| + (|\bar{B}_1| - |B_1|) + (|\bar{B}_2| - |B_2|),$$

hence, due to the assumptions, we obtain

$$|A_1 \cap A_2| \leq |\pi(Z_1) \cap \pi(Z_2)| + (|A_1| - |\pi(Z_1)|) + (|A_2| - |\pi(Z_2)|).$$

We have already proved that $|\pi(Z_1) \cap \pi(Z_2)| = |Z_1 \cap Z_2|$. Moreover, from the definition of $\pi(Z_i)$ it is obvious that $|\pi(Z_i)| = |Z_i|$. Hence, we obtain the second inequality. \square

We are ready for the proof of the main theorem of Section 4.

Proof of Theorem 4.5. By Lemma B.1

$$\begin{aligned}
 |\pi(i) - \pi(j)| &= \frac{1}{2} \left| \left(\pi(i) + C(l_i^{(\pi)}) \right) \triangle \left(\pi(j) + C(l_j^{(\pi)}) \right) \right| \\
 &= \frac{1}{2} \left(2l_i^{(\pi)} + 1 - \left| \left(\pi(i) + C(l_i^{(\pi)}) \right) \cap \left(\pi(j) + C(l_j^{(\pi)}) \right) \right| \right. \\
 &\quad \left. + 2l_j^{(\pi)} + 1 - \left| \left(\pi(i) + C(l_i^{(\pi)}) \right) \cap \left(\pi(j) + C(l_j^{(\pi)}) \right) \right| \right) \\
 &= l_i^{(\pi)} + l_j^{(\pi)} + 1 - \left| \left(\pi(i) + C(l_i^{(\pi)}) \right) \cap \left(\pi(j) + C(l_j^{(\pi)}) \right) \right|.
 \end{aligned}
 \tag{B.4}$$

On the other hand, by Lemma B.2, for $Z_1 = D_i, Z_2 = D_j, A_1 = \pi(i) + C(l_i^{(\pi)})$ and $A_2 = \pi(j) + C(l_j^{(\pi)})$:

$$\begin{aligned}
 |D_i \cap D_j| &\leq \left| \left(\pi(i) + C(l_i^{(\pi)}) \right) \cap \left(\pi(j) + C(l_j^{(\pi)}) \right) \right| \\
 \left| \left(\pi(i) + C(l_i^{(\pi)}) \right) \cap \left(\pi(j) + C(l_j^{(\pi)}) \right) \right| &\leq |D_i \cap D_j| + 2l_i^{(\pi)} - |D_i| + 2l_j^{(\pi)} - |D_j| + 2.
 \end{aligned}$$

Using (B.4) and the above inequalities, we obtain upper and lower bounds

$$|\pi(i) - \pi(j)| \leq l_i^{(\pi)} + l_j^{(\pi)} - |D_i \cap D_j| + 1, \tag{B.5}$$

$$|\pi(i) - \pi(j)| \geq |D_i| + |D_j| - |D_i \cap D_j| - l_i^{(\pi)} - l_j^{(\pi)} - 1. \tag{B.6}$$

Simple algebra leads to the following

$$-\frac{U-L}{2} \leq |\pi(i) - \pi(j)| - \frac{U+L}{2} \leq \frac{U-L}{2}, \tag{B.7}$$

where U and L are the right-hand side of (B.5) and (B.6), respectively. Moreover, $U+L = |D_i \triangle D_j| = 2(\mathbf{A}_\Sigma)_{ij}$ and $U-L = 2l_i^{(\pi)} + 2l_j^{(\pi)} + 2 - |D_i| - |D_j|$. This ends the proof of the theorem. \square

Proof of Proposition 4.11. Due to the assumptions, we can apply the inequalities (4.7) to the formula (4.4). Furthermore, since \mathbf{G}_π and \mathbf{A}_Σ are distance matrices, hence $[\mathbf{G}_\pi]_{ii} = [\mathbf{A}_\Sigma]_{ii} = 0$ for all i and

$$\begin{aligned}
 \delta_m(\mathbf{G}_\pi, \mathbf{A}_\Sigma) &\leq \frac{1}{dm} \sum_{\substack{i \neq j \\ [\mathbf{G}_\pi]_{ij} \leq m}} \left(\frac{2l_i^{(\pi)} + 1 - |D_i|}{2} + \frac{2l_j^{(\pi)} + 1 - |D_j|}{2} \right) \\
 &= \frac{1}{dm} \sum_{i=1}^d \left(2l_i^{(\pi)} + 1 - |D_i| \right) \sum_{j=1}^d \mathbb{I}(j \neq i, |\pi(i) - \pi(j)| \leq m) \\
 &= \frac{1}{dm} \sum_{i=1}^d \left(2l_i^{(\pi)} + 1 - |D_i| \right) \left| (\{1, \dots, d\} \cap (\pi(i) + C(m))) \setminus \{\pi(i)\} \right| \\
 &= \frac{2}{d} \sum_{i=1}^d (2l_i^{(\pi)} + 1 - |D_i|) - \frac{1}{d} \sum_{\pi(i)=1}^m \frac{m+1-\pi(i)}{m} (2l_i^{(\pi)} + 1 - |D_i|) \\
 &\quad - \frac{1}{d} \sum_{\pi(i)=d-m+1}^d \frac{m-d+\pi(i)}{m} (2l_i^{(\pi)} + 1 - |D_i|).
 \end{aligned}$$

In the last equation, we used a fact that for $\pi(i) \in \{1, \dots, m\} \cup \{d-m+1, \dots, d\}$ the number of neighbors linearly decreases as $\pi(i)$'s approach the endpoints 1 and d . \square

B.3. Proofs of Section 5. For a 0–1 symmetric matrix $\mathbf{A} = [\mathbf{A}_{i,j}]$, $l_i(\mathbf{A})$ is the half-width of the set D_i associated with the matrix \mathbf{A} under the identity permutation.

To prove Theorem 5.1, we need the following lemma that describes the relationship between the half-widths of two matrices that differ by a single nonzero element (along with its symmetric counterpart). Moreover, it specifies the effect of zeroing out the elements farthest from the diagonal in the initial matrix.

LEMMA B.3. *Let λ be the half-bandwidth of a symmetric $d \times d$ matrix \mathbf{A} . For $i \in \{1, \dots, d-1\}$ and $k \in \{1, \dots, d-i\}$, let $\mathbf{A}_{i,i+k}$ and $\mathbf{A}_{i+k,i}$ be nonzero and \mathbf{B} be obtained from \mathbf{A} by setting these entries to zero. Then*

$$(B.8) \quad \|\mathbf{l}(\mathbf{A})\|_1 - \|\mathbf{l}(\mathbf{B})\|_1 = l_i(\mathbf{A}) - l_i(\mathbf{B}) + l_{i+k}(\mathbf{A}) - l_{i+k}(\mathbf{B}) \geq 0.$$

If $k = \lambda$, then

- i) $l_i(\mathbf{A}) - l_i(\mathbf{B}) \geq 1$, whenever $\mathbf{A}_{i,i-\lambda} = 0$ or $i \leq \lambda$, with the equality holding if, additionally, $\mathbf{A}_{i,i+\lambda-1} = 1$ or $\mathbf{A}_{i-\lambda+1} = 1$,
- ii) $l_{i+\lambda}(\mathbf{A}) - l_{i+\lambda}(\mathbf{B}) \geq 1$, whenever $\mathbf{A}_{i+\lambda,i+2\lambda} = 0$ or $i+2\lambda > d$, with the equality holding if, additionally, $\mathbf{A}_{i+\lambda,i+1} = 1$ or $\mathbf{A}_{i+\lambda,i+2\lambda-1} = 1$.

A rather straightforward proof of the above fact is omitted.

For a symmetric 0–1 matrix \mathbf{A} with the half-bandwidth $\lambda \geq 1$, let $j = \min\{i \mid l_i(\mathbf{A}) = \lambda\}$ and $m(\mathbf{A})$ be the largest positive integer m for which

$$\mathbf{A}_{j+(t-1)\lambda, j+t\lambda} = 1, \quad t = 1, \dots, m.$$

It is clear that either $\mathbf{A}_{j+m\lambda, j+(m+1)\lambda} = 0$ or $j + (m(\mathbf{A}) + 1)\lambda > d$.

The sequence of pairs of indices

$$S(\mathbf{A}) = (j, j) + \lambda \cdot ((0, 1), (1, 2), \dots, (m(\mathbf{A}) - 1, m(\mathbf{A})))$$

describes the first longest contiguous sequence of 1 along the band, with each element corresponding to an entry in \mathbf{A} spaced exactly λ positions apart in row (and column) indices, terminating at either a zero or the matrix boundary.

COROLLARY B.4. *Let \mathbf{A} have the half-bandwidth $\lambda \geq 1$. Consider the matrix \mathbf{B} obtained from \mathbf{A} by zeroing out all 1's on the boundary given through $S(\mathbf{A})$ together with their symmetric counterparts. Then*

$$\|\mathbf{l}(\mathbf{A})\|_1 - \|\mathbf{l}(\mathbf{B})\|_1 \geq m(\mathbf{A}) + 1$$

and the equality holds if for each $(i, j) \in S(\mathbf{A})$, $\mathbf{A}_{i,j-1} = \mathbf{A}_{i+1,j} = 1$.

Proof. The proof reduces to an iterative application of Lemma B.3 in the case when $k = \lambda$. Let us define the initial matrix as $\mathbf{A}^{(0)} = \mathbf{A}$. In each iteration step t , the matrix $\mathbf{A}^{(t)}$ is obtained from $\mathbf{A}^{(t-1)}$ by zeroing the entry indexed by the last element in $S(\mathbf{A}^{(t-1)})$ (and its symmetric counterpart). Clearly, $S(\mathbf{A}^{(t)})$ is a sequence consisting of the first $m - t$ elements of the sequence $S(\mathbf{A}^{(0)})$. Hence, $\mathbf{A}^{(m)} = \mathbf{B}$.

Due to the construction of the sets $S(\mathbf{A}^{(t)})$, it is straightforward to show that for all $t < m$, the weaker assumption in ii) of Lemma B.3 is satisfied for the element indexed by the last entry in $S(\mathbf{A}^{(t)})$. Therefore, using (B.8), we reduce by at least 1

of the half-width at each step. In the case when $t = m$, the weaker assumptions of both *i*) and *ii*) hold, resulting in a reduction by at least 2. Naturally, when for each $(i, j) \in S(\mathbf{A})$, $\mathbf{A}_{i,j-1} = \mathbf{A}_{i+1,j} = 1$, then the stronger assumptions of *i*) and *ii*) hold at each step, and we obtain the equality. \square

Proof of Theorem 5.1. Corollary B.4, applied iteratively, allows us to establish a lower bound for the half-width of any symmetric matrix Σ . Let $\Sigma^{(0)} = \Sigma$. At step t , $\Sigma^{(t)}$ correspond to \mathbf{B} in the corollary in which we take $\mathbf{A} = \Sigma^{(t-1)}$. It is clear that the procedure can be carried out until there is no nonzero terms outside the diagonal and this terminating step is denoted by \tilde{t} , for which $\|\mathbf{l}(\Sigma^{(\tilde{t})})\|_1 = 0$. Thus

$$(B.9) \quad \|\mathbf{l}(\Sigma^{(0)})\|_1 \geq \tilde{t} + \sum_{i=0}^{\tilde{t}-1} m(\Sigma^{(i)}) = \tilde{t} + |\{(i, j) : \Sigma_{ij} \neq 0, i < j\}|,$$

since the iterative procedure eliminates all off-diagonal elements of $\Sigma^{(0)}$. Furthermore, if $\Sigma^{(0)}$ is a full band matrix, then

$$(B.10) \quad \|\mathbf{l}(\Sigma^{(0)})\|_1 = \tilde{t} + |\{(i, j) : \Sigma_{ij} \neq 0, i < j\}|$$

since the additional assumptions in *i*) and *ii*) of Lemma B.3 are always fulfilled.

From (B.9), it follows that the lower bound on the half-width is determined by two factors: (1) the number of nonzero off-diagonal elements in the matrix; (2) the number of iterations required to transform it into a diagonal matrix. The key factor in determining whether a given permutation is optimal is the number of iterations, since row and column permutations do not alter the total count of nonzero elements.

The number of iterations \tilde{t} is minimized, when the sequences $S(\Sigma^{(i)})$ are as long as possible. The length of each sequence depends on two key parameters: the half-bandwidth λ_i and the number of available positions on the subdiagonal at order λ_i . The parameter λ dictates the row-wise separation between consecutive elements in $S(\Sigma^{(i)})$. Meanwhile, the subdiagonal at order λ contains $d - \lambda$ elements. Consequently, the maximum possible length $m(\Sigma^{(i)})$ is a decreasing function of λ_i , since a larger λ_i leaves fewer elements available for placement and increases the distance between consecutive elements in the sequence. From this reasoning, combined with (B.10), we conclude that among all matrices with the number of nonzero off-diagonal elements equal to the number in a full band matrix, the full band matrix configuration requires the minimal number of iterations. This proves the Theorem 5.1. \square

Proof of Theorem 5.3. The part *i*) is a rather standard observation due to the connection between $\Sigma(t)$ and the matrix Σ^t and noticing that for a matrix \mathbf{A} and a permutation matrix $\tilde{\pi}$:

$$\left(\tilde{\pi}^\top \mathbf{A} \tilde{\pi}\right)^t = \tilde{\pi}^\top \mathbf{A}^t \tilde{\pi}.$$

In order to prove *ii*) and *iii*), it is enough to consider properties of a $d \times d$ full band matrix with half-bandwidth $\lambda \geq 1$. Under *ii*), there are only two rows having $\lambda + 1$ nonzero elements (the first and the last in the original not-permuted band matrix), so that there are two options to have such a row as the first row. However, all the other rows have to be chosen in a unique way and with the agreement with the original order, when the originally first row is put as the first row or in the reverse order, when the originally last row is put as the first one.

To show *iii*), we note that there are only two choices of setting the first $d - \lambda - 1$ rows and the last $d - \lambda - 1$ rows, by the same argument as before. The remaining

$2\lambda + 2 - d$ rows at the center have all entries nonzero and thus any permutation between them will not change the nonzero terms in the rest of the matrix. Finally, the last relation is because the full central rows that can be arbitrarily permuted for $\Sigma(t)$ constitute a subset of those that correspond to $\Sigma(t + 1)$. \square

Acknowledgments. The second and third authors have been partially supported by the Swedish Research Council (VR) Grant DNR: 2020-05168.

REFERENCES

- [1] I. BORG AND P. GROENEN, *Modern Multidimensional Scaling: Theory and Applications (Springer Series in Statistics)*, Springer, 08 2005.
- [2] U. BRANDES AND C. PICH, *Eigensolver methods for progressive multidimensional scaling of large data*, in Graph Drawing, M. Kaufmann and D. Wagner, eds., Berlin, Heidelberg, 2007, Springer Berlin Heidelberg, pp. 42–53.
- [3] L. CAMBIER, C. CHEN, E. G. BOMAN, S. RAJAMANICKAM, R. S. TUMINARO, AND E. DARVE, *An algebraic sparsified nested dissection algorithm using low-rank approximations*, SIAM Journal on Matrix Analysis and Applications, 41 (2020), pp. 715–746, <https://doi.org/10.1137/19M123806X>.
- [4] V. DE SILVA AND J. B. TENENBAUM, *Sparse multidimensional scaling using land-mark points*, tech. report, Technical Report, Stanford University, 2004, <https://api.semanticscholar.org/CorpusID:16670256>.
- [5] P. DELICADO AND C. PACHÓN-GARCÍA, *Multidimensional scaling for big data*, Advances in Data Analysis and Classification, (2024).
- [6] C. FALOUTSOS AND K.-I. LIN, *Fastmap: a fast algorithm for indexing, data-mining and visualization of traditional and multimedia datasets*, in Proceedings of the 1995 ACM SIGMOD International Conference on Management of Data, SIGMOD '95, New York, NY, USA, 1995, Association for Computing Machinery, pp. 163–174, <https://doi.org/10.1145/223784.223812>.
- [7] A. GEORGE, *Nested dissection of a regular finite element mesh*, SIAM Journal on Numerical Analysis, 10 (1973), pp. 345–363, <https://doi.org/10.1137/0710032>.
- [8] J. R. GILBERT AND R. E. TARJAN, *The analysis of a nested dissection algorithm*, Numerische Mathematik, 50 (1986), pp. 377–404, <https://doi.org/10.1007/BF01396660>.
- [9] J. C. GOWER, *Some distance properties of latent root and vector methods used in multivariate analysis*, Biometrika, 53 (1966), pp. 325–338.
- [10] J. GRGAR, *How ordinary elimination became gaussian elimination*, Historia Mathematica, 38 (2011), pp. 163–218.
- [11] R. W. HOCKNEY, *The Science of Computer Benchmarking*, Software, Environments, Tools, Society for Industrial and Applied Mathematics, 1996.
- [12] S. J. LEON, Å. BJÖRCK, AND W. GANDER, *Gram-Schmidt orthogonalization: 100 years and more*, Numerical Linear Algebra with Applications, 20 (2013), pp. 492–532.
- [13] R. J. LIPTON, D. J. ROSE, AND R. E. TARJAN, *Generalized nested dissection*, SIAM Journal on Numerical Analysis, 16 (1979), pp. 346–358, <https://doi.org/10.1137/0716027>.
- [14] C. H. PAPADIMITRIOU, *The np -completeness of the bandwidth minimization problem*, Computing, 16 (1976), pp. 263–270.
- [15] E. PARADIS, *Reduced multidimensional scaling*, Computational Statistics, 37 (2022), pp. 91–105.
- [16] L. PURSELL AND S. TRIMBLE, *Gram-Schmidt orthogonalization by Gauss elimination*, The American Mathematical Monthly, 98 (1991), pp. 544–549.
- [17] D. J. ROSE, *A graph-theoretic study of the numerical solution of sparse positive definite systems of linear equations*, in Graph theory and computing, Elsevier, 1972, pp. 183–217.
- [18] W. S. TORGERSON, *Multidimensional scaling: I. theory and method*, Psychometrika, 17 (1952), pp. 401–419.
- [19] L. N. TREFETHEN AND D. BAU, *Numerical Linear Algebra*, Society for Industrial and Applied Mathematics, 1997.
- [20] C. WANG, C. XU, AND A. LISSER, *Bandwidth minimization problem*, 2014, <https://api.semanticscholar.org/CorpusID:125789981>.
- [21] J. WANG, X. WANG, K.-I. LIN, D. SHASHA, AND B. SHAPIRO, *Evaluating a class of distance mapping algorithms for data mining and clustering*, in Proceedings of the international conference on knowledge discovery and data mining, San Diego, California, August 1999, 1999.

- [22] T. YANG, J. LIU, L. McMILLAN, AND W. WANG, *A fast approximation to multidimensional scaling*, in IEEE Workshop on computation intensive methods for computer vision, 2006.